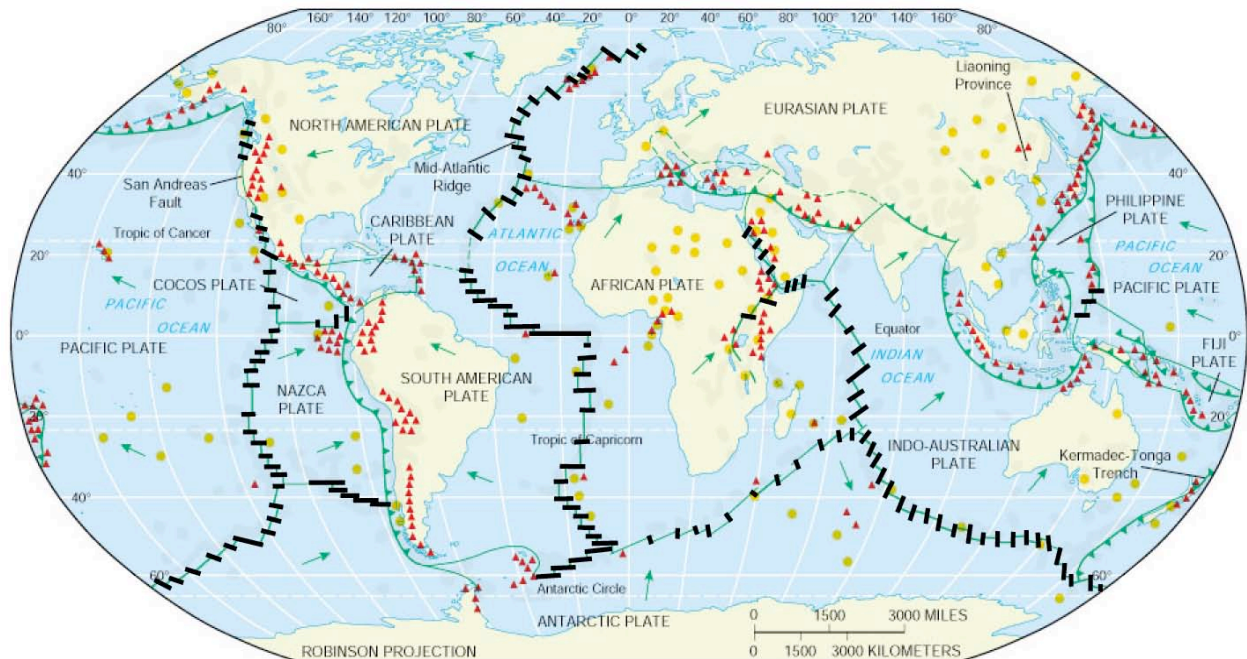


# Understanding Earth's major volcanic systems

First we will focus on mid-ocean ridges



- ▲ volcanoes
- hot spots
- oceanic transform fault
- divergent boundary
- ▼ convergent boundary
- motion vector

<http://www.usgs.gov>

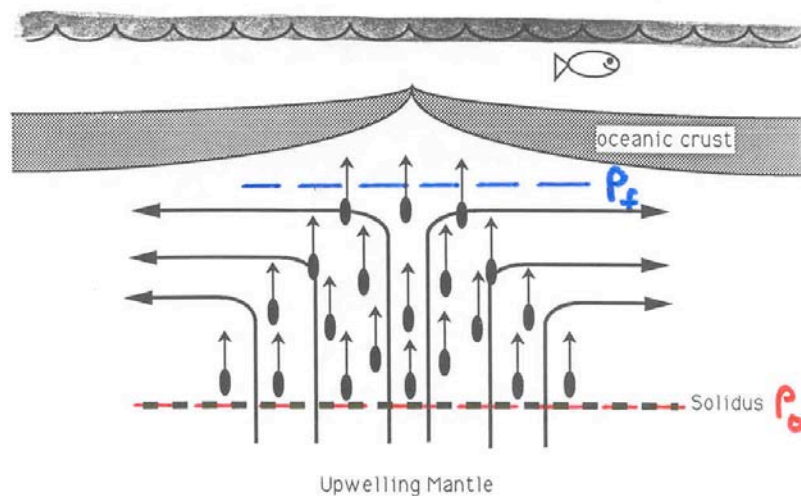
The data comes from compositions of mid-ocean ridge basalts obtained by dredging or direct sampling from the ocean floor.  
ALVIN – East Pacific Rise dive 1999



Drained sheet flow on the EPR – notice columns – created by boiling of seawater trapped beneath the flow – chilled crust is supported by these features – lava beneath crust flows out on to flanks forming fields of pillows -

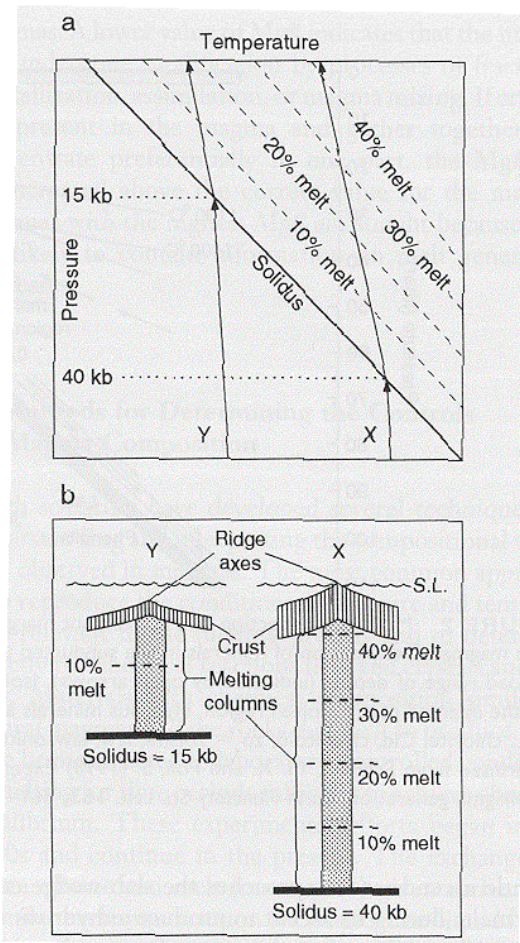
Scale column = 3 meters

26 11 15



Constraints from Experimental Petrology on Mantle Melting Variations:

- (1) Mantle temperature
- (2) Pressure range of Melting
- (3) Extent of melting
- (3) Style of melting process (near-fractional, batch)
- (4) Composition of the source



Adiabatic decompression melting beneath mid-ocean ridges.

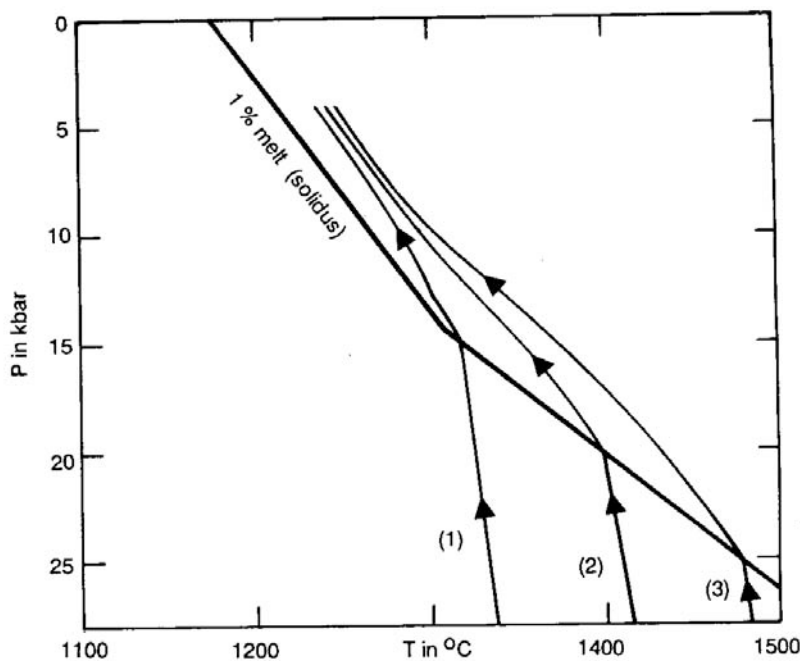
Leads to a mean depth and mean temperature of melt extraction.

$$P_m = (P_0 - P_{fin})/2 + P_{fin}$$

Melting is near-fractional.

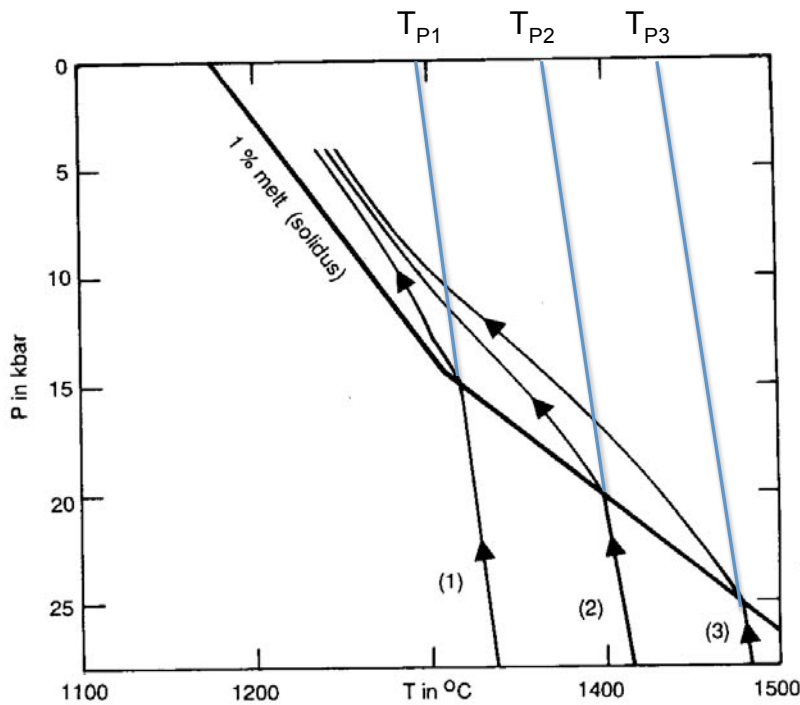
Mantle cools as it melts.

Klein & Langmuir (1987)



Adiabatic decompression melting – all of the superheat obtained from the extension of the adiabat above the melting curve is turned into heat of fusion. Three calculated melting paths are shown here for three different melting models.

Kinzler & Grove (1992)



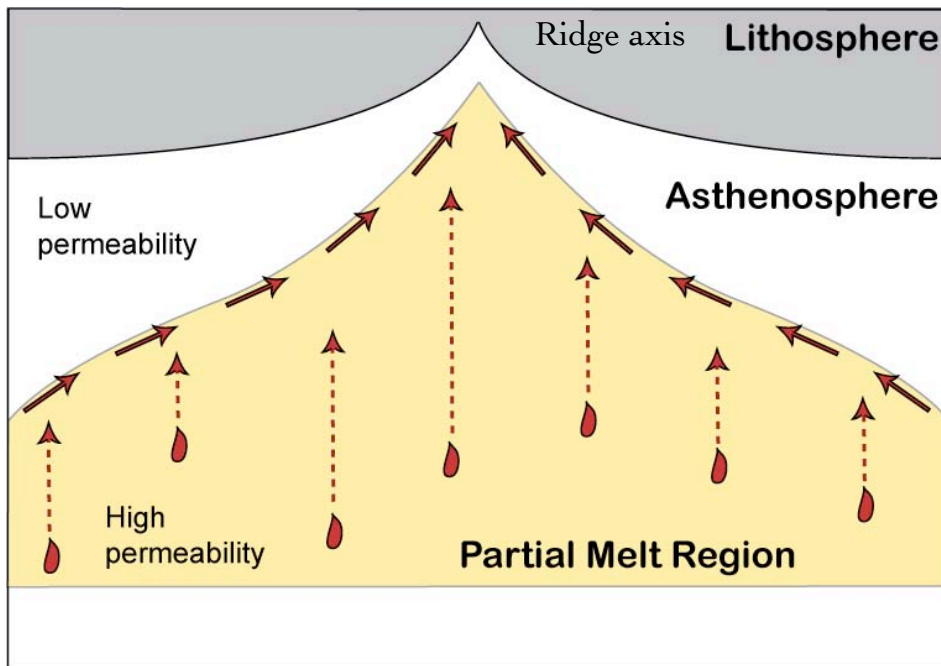
Potential temperatures for MORB are defined as the temperature of the beginning of melting projected along an adiabatic gradient to the Earth's surface.

Shown here by blue lines

Adiabat  $\sim 10^\circ\text{C}/\text{GPa}$

Kinzler & Grove (1992)

## Melt Migration

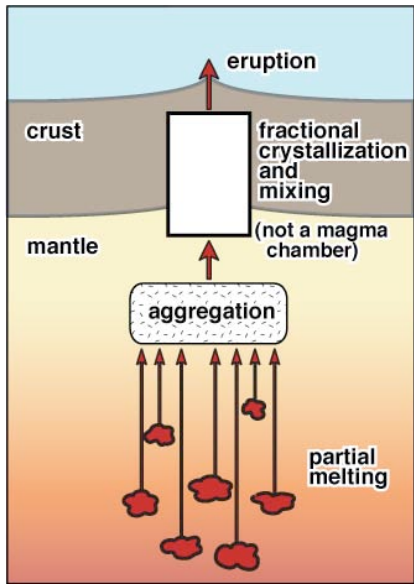


The melting regime beneath mid-ocean ridges is "shaped" and melt is focused toward the ridge axis and pooled.

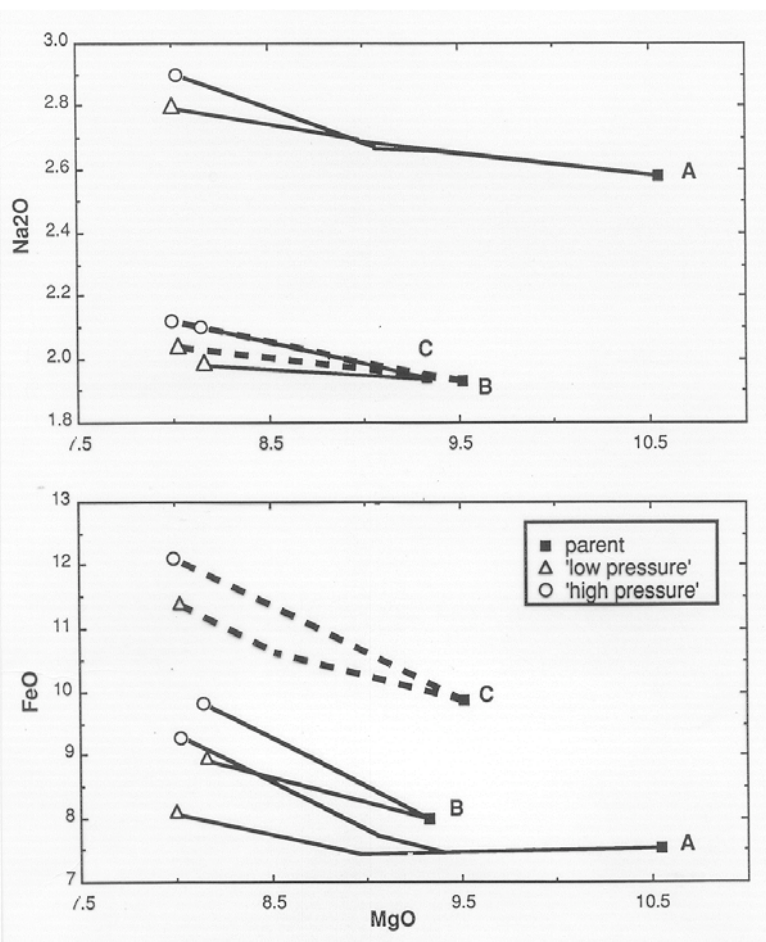
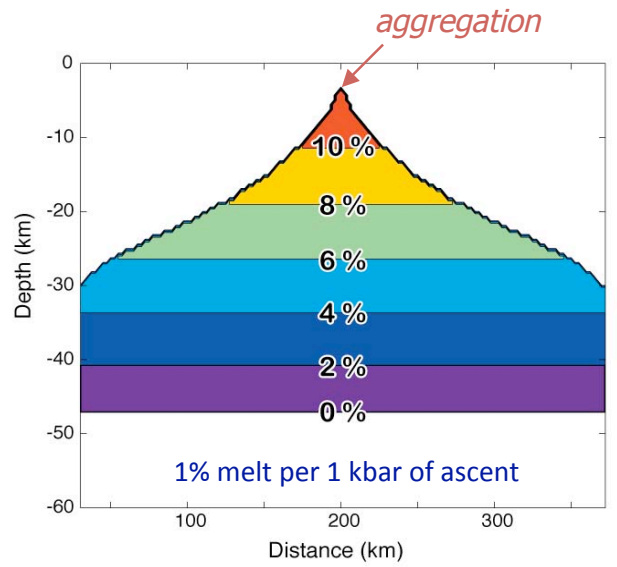
Adapted from Sparks and Parmentier, *EPSL* (1991)

## Melt model calculations:

- (1) Near fractional melting, Kinzler & Grove (1992a,b, and 1993)
- (2) Pooling of melt (aggregation)
- (3) Fractional crystallization, Yang et al. (1996)



Grove et al. (1992)

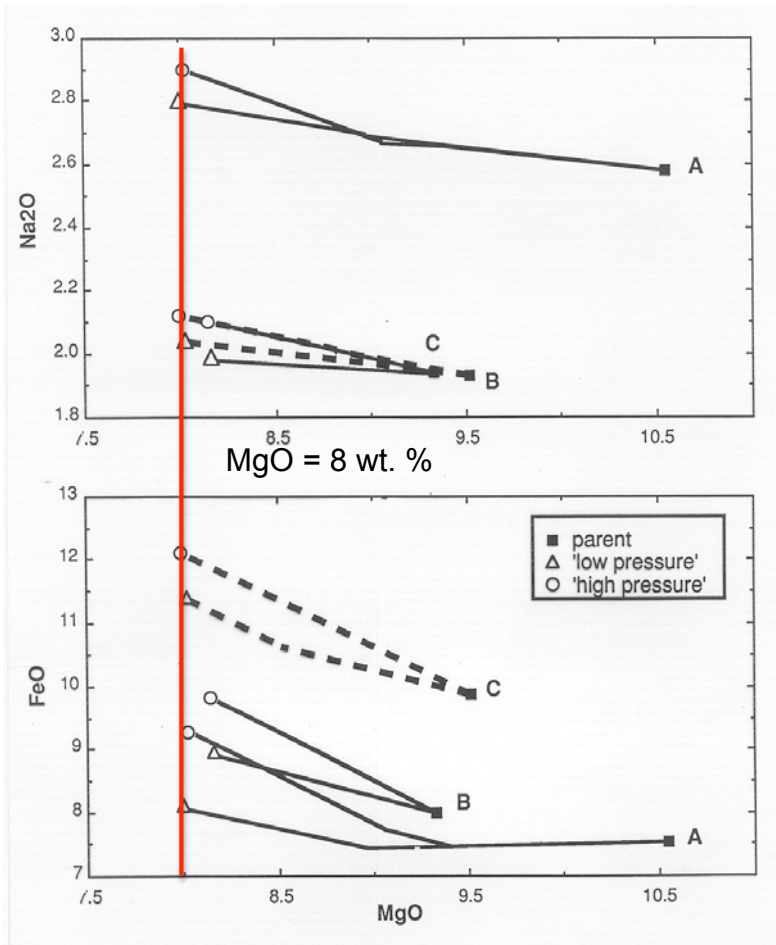


A, B and C are pooled near-fractional melts from 3 different  $T_p$ 's.

These variation diagrams show Na<sub>2</sub>O and FeO plotted against MgO, and the 2 paths represent fractional crystallization (F.C.) processes imposed at different pressures. The depth (pressure) of F.C. depths on the thermal structure of the oceanic lithosphere.

Lithosphere Temperature is imposed by spreading rate and hydrothermal cooling.

Grove et al. (1992)

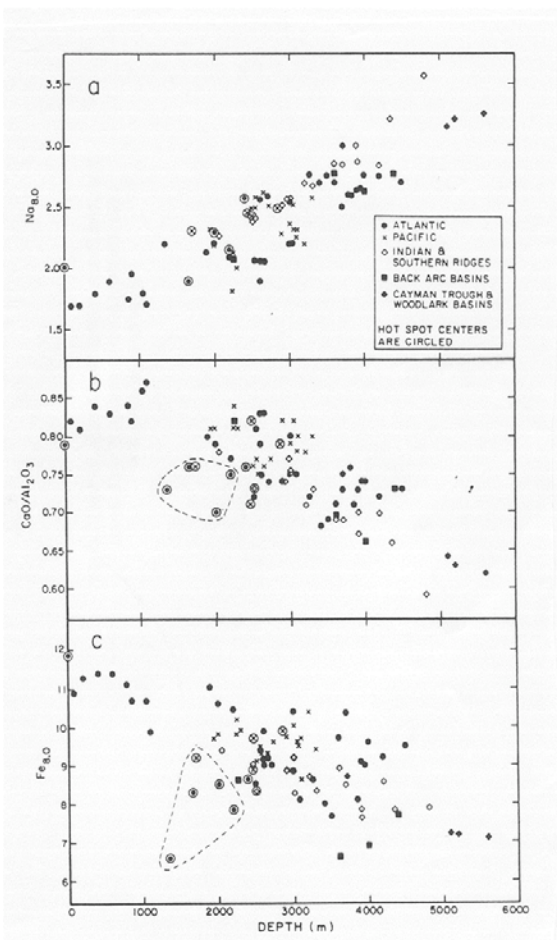


A, B and C are pooled near-fractional melts from 3 different  $T_p$ 's.

These variation diagrams show  $\text{Na}_2\text{O}$  and  $\text{FeO}$  plotted against  $\text{MgO}$ , and the 2 paths represent fractional crystallization (F.C.) processes imposed at different pressures. The depth (pressure) of F.C. depths on the thermal structure of the oceanic lithosphere.

Lithosphere Temperature is imposed by spreading rate and hydrothermal cooling.

Grove et al. (1992)



Global MORB data from Klein and Langmuir (1987) shows correlation of MORB composition with depth to ridge

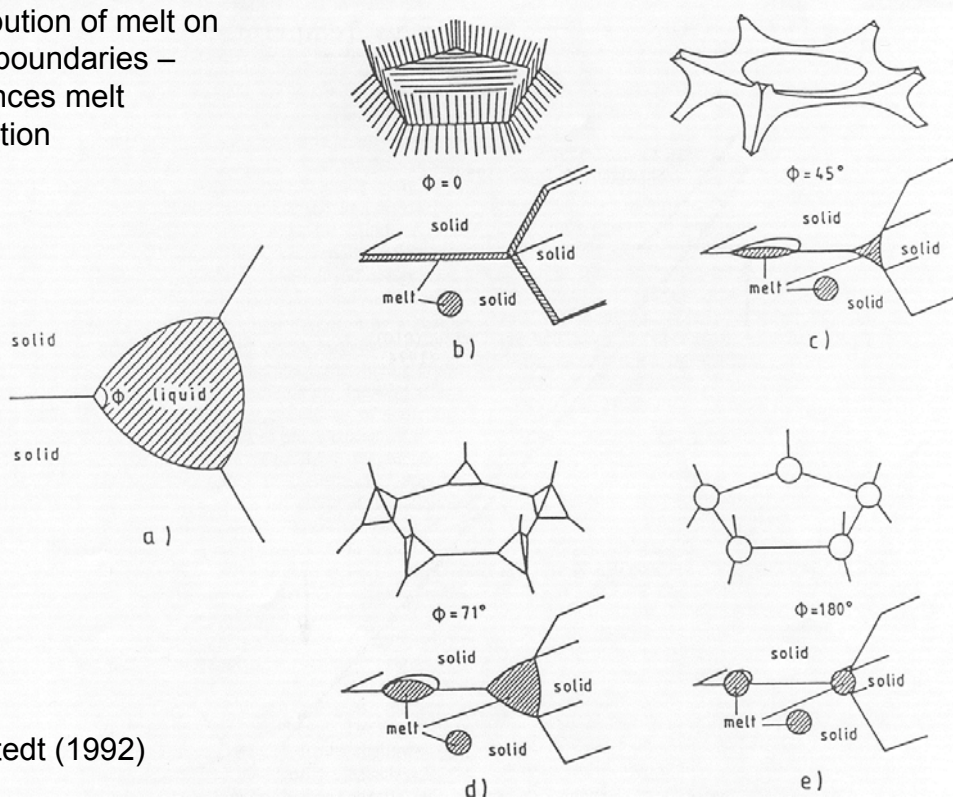
Implies a relation between MORB melting process and mantle potential temperature

Where shallower depth to ridge = higher temperature = increased thermal buoyancy

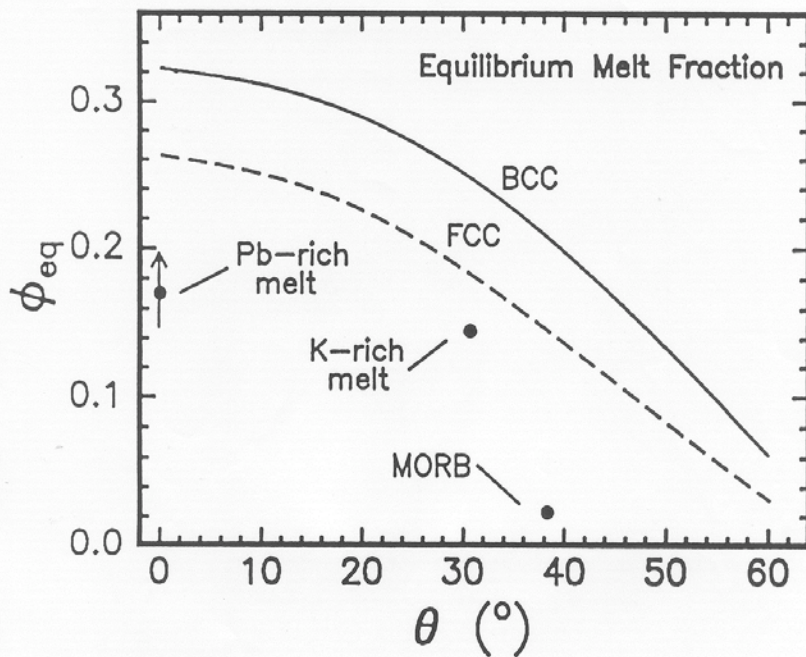
Greater depth = lower temperature = less buoyancy in ascending mantle

Klein & Langmuir (1992)

Distribution of melt on grain boundaries – influences melt extraction



Kohlstedt (1992)



Kohlstedt (1992)

Fig. 2. Equilibrium melt fraction,  $\phi_{eq}$ , as a function of dihedral angle,  $\theta$ ,

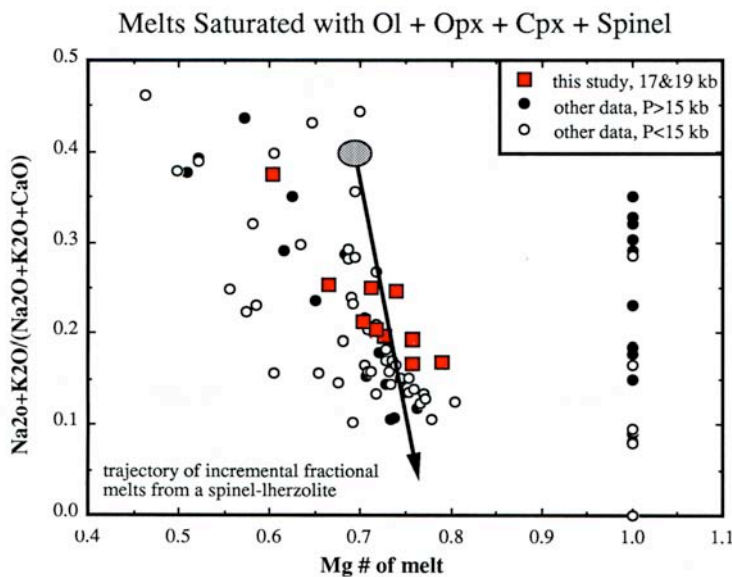
Very low melt fraction left in mantle residue – implies that MORB melting is near fractional – melt is removed as it is produced

# Piston Cylinder



Our mantle melting model is calibrated by direct experimental determination of liquids saturated with the mantle residual assemblage:

Olivine + Orthopyroxene + Clinopyroxene + Aluminous Phase (Plagioclase, Spinel or Garnet)



To calibrate a melting model for MORB we require direct experimental data from natural basalt melts that are multiply saturated with the four phases present in lherzolite:

Olivine + Orthopyroxene + Clinopyroxene + Spinel  
or  
Oliv + Opx + Cpx + Plagioclase  
or  
Oliv + Opx + Cpx + Garnet

**Data Sources:**

Walter and Presnall, submitted  
Kinzler and Grove (1992)  
Falloon and Green (1987, 1988)  
Fujii and Scarfe (1985)  
Elthon and Scarfe (1984)

This is the data set used by Kinzler (1997).

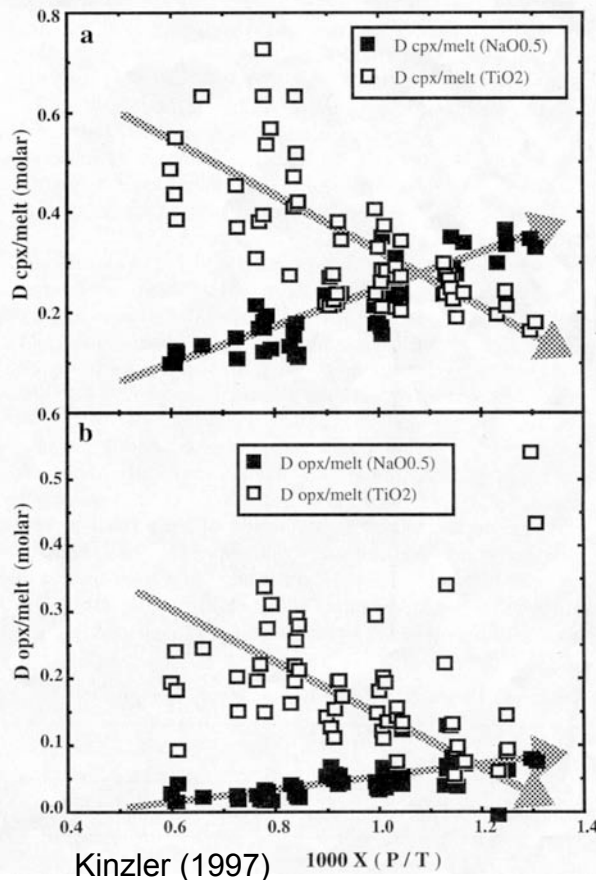
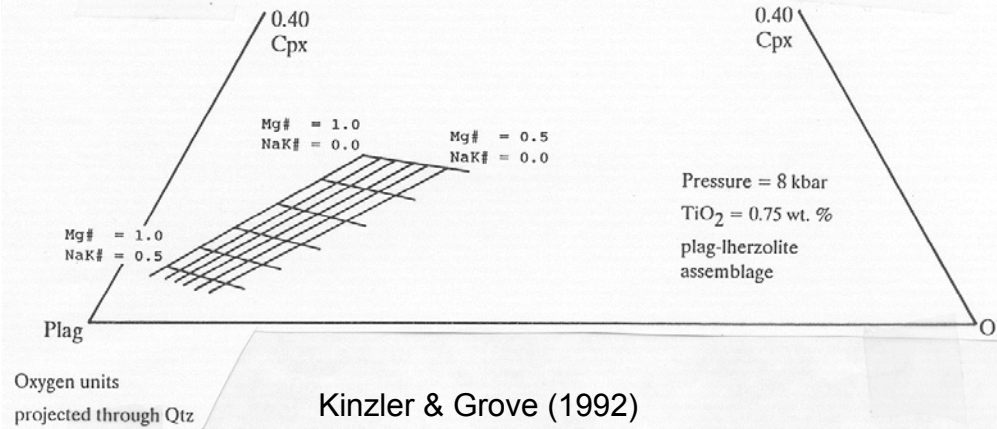
							$R^2$			
T	= 1242	+ 9	(P-0.001)	+ -120	(1-mg#)	+ -88.8	A#	+ -6.6	TiO <sub>2</sub>	0.88
OI	= .120	+ .008	(P-0.001)	+ .229	(1-mg#)	+ -.335	A#	+ -.009	TiO <sub>2</sub>	0.97
Cpx	= .261	+ -.008	(P-0.001)	+ -.069	(1-mg#)	+ -.104	A#	+ .012	TiO <sub>2</sub>	0.95
Pl	= .419	+ .012	(P-0.001)	+ -.135	(1-mg#)	+ .691	A#	+ .000	TiO <sub>2</sub>	0.95
Qz	= .200	+ -.012	(P-0.001)	+ .000	(1-mg#)	+ -.252	A#	+ .000	TiO <sub>2</sub>	0.97

A model for predicting the melts saturated with:

Oliv + Opx + Cpx + Plag

from Kinzler and Grove (1992)

Projection scheme shows systematic effects of key variables that control melt composition.

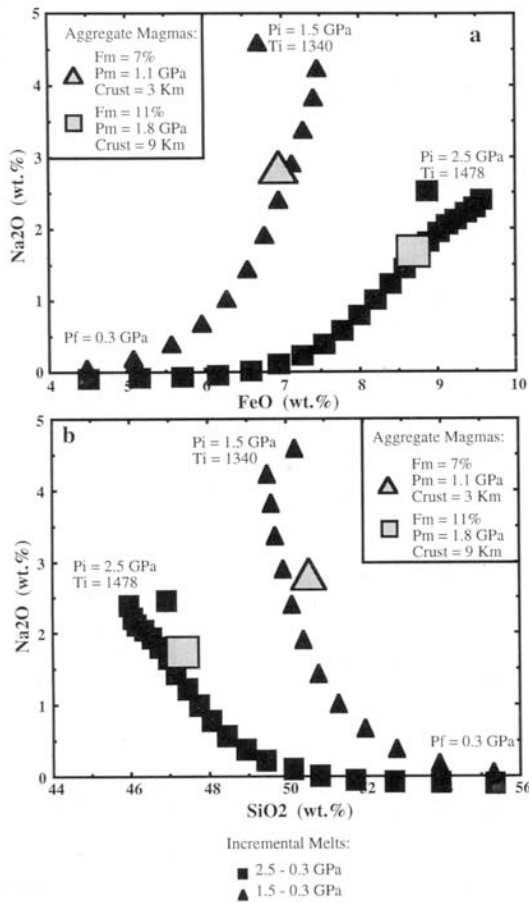


The K&G (1992) and Kinzler (1997) models are inspired by the Gibbs method and calculate the composition of a liquid in equilibrium with a mantle residual assemblage.

The model keeps track of the change in the bulk composition of the solid mantle residue as it evolves during progressive fractional melting.

Mass balance calculations:

- Mg# of the solids and  $K_{D_{Fe-Mg}}$  are used to calculate the major element compositions of the residue.
- $K_d$ 's for Na<sub>2</sub>O, TiO<sub>2</sub> and Al<sub>2</sub>O<sub>3</sub> of clinopyroxene and orthopyroxene calculate the minor components.
- CaO of pyroxenes is estimated from an experimentally determined 2-phase region.



Examples of polybaric, near fractional melting models from Kinzler (1997).

These two models bracket the global variability observed in MORB suites.

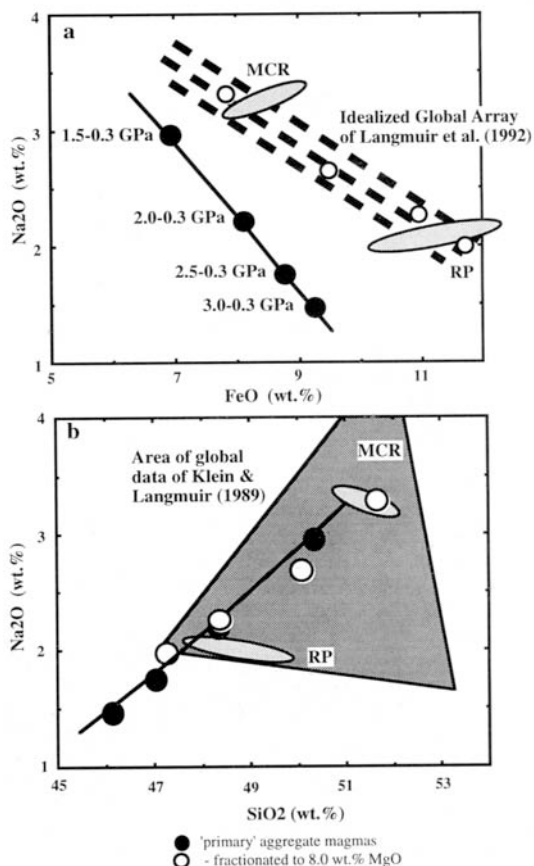
Small triangles indicate fractional melts where each melt increment is ~ 1 wt. %.

The lower  $T_P$  case starts at shallower pressures.

The higher  $T_P$  case begins at greater pressures.

Note differences in melting extent and the difference in the aggregated melt compositions (large grey triangles).

Kinzler (1997)



The same data shown "corrected" to  $MgO_{8.0}$  for a range of pressures of fractional crystallization (grey ellipses).

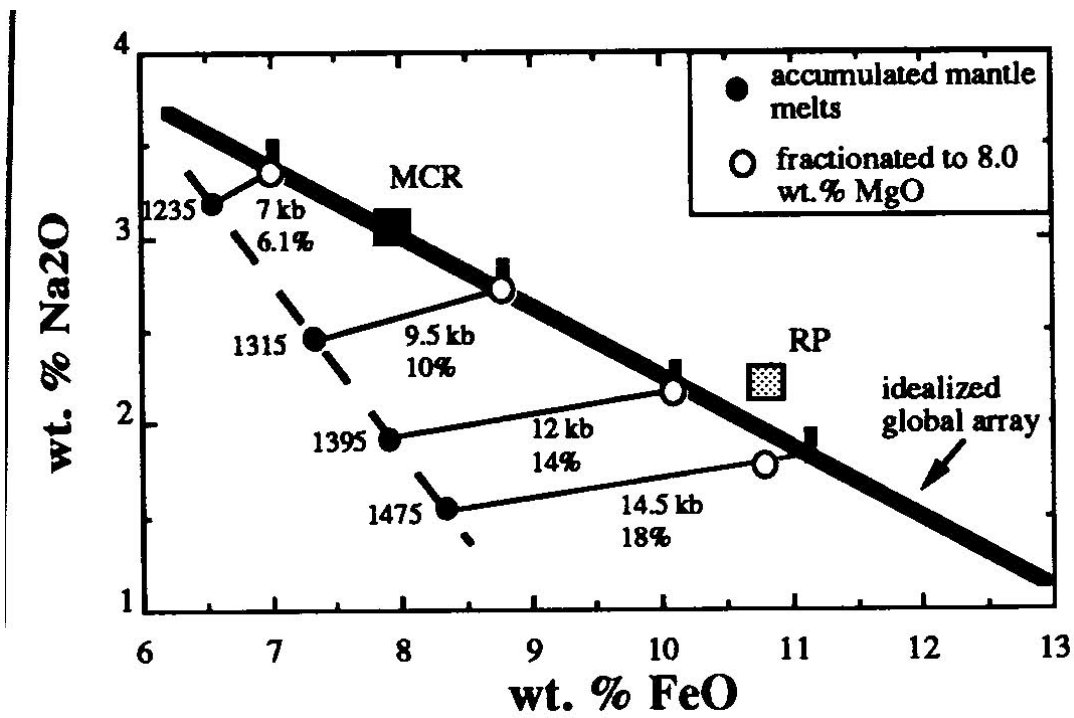
Black circles = primary mantle melts produced by polybaric, near-fractional adiabatic decompression melting.

Dashed lines show the position of the global MORB array.

MCR = mid-Cayman Rise

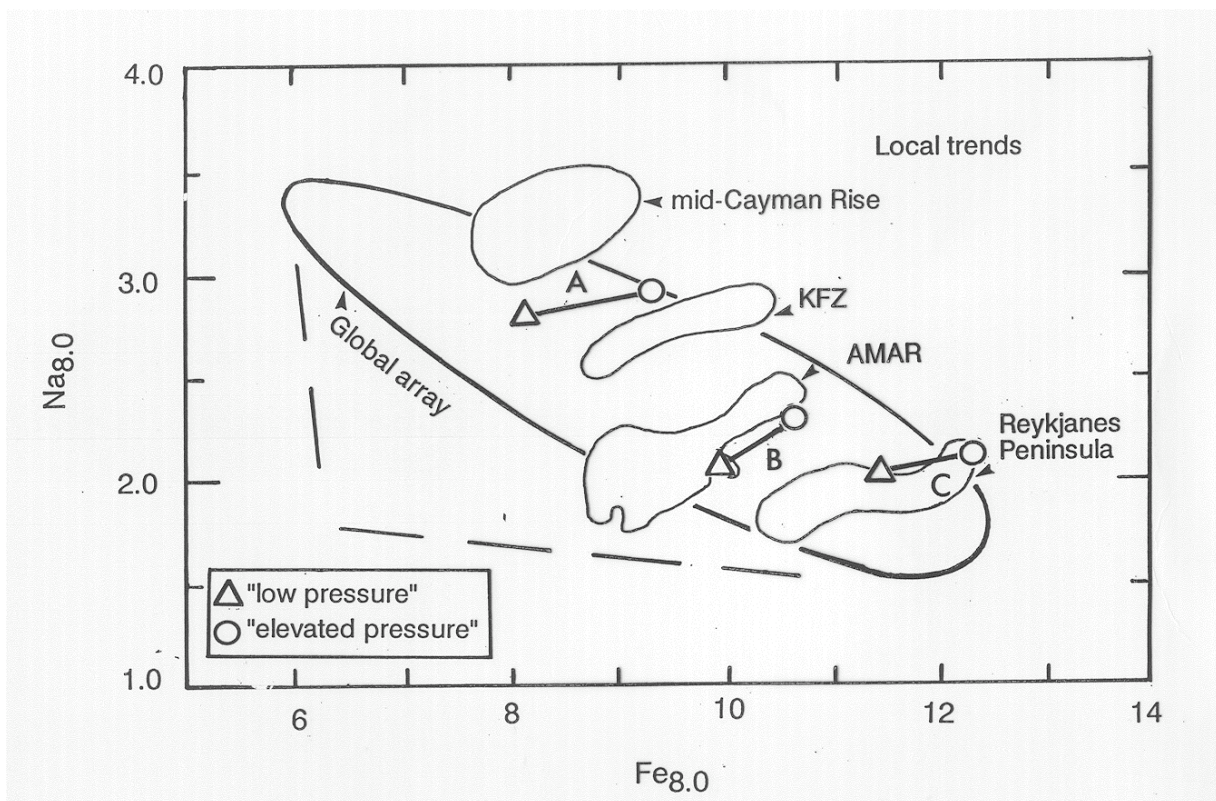
RP = Reykjanes Pensinsula

Kinzler (1997)



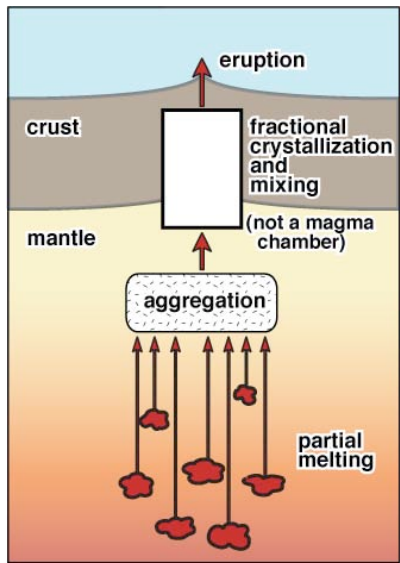
Melting models corrected for fractional crystallization plotted on  $\text{Na}_8$  vs.  $\text{Fe}_8$  projection of Langmuir et al. (1992).

Kinzler and Grove (1993)

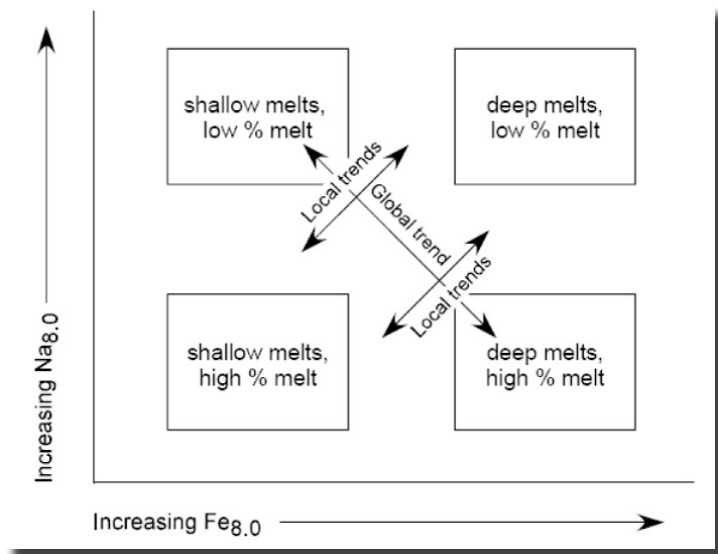


Melting models plotted on  $\text{Na}_8$  vs.  $\text{Fe}_8$  projection of Langmuir et al. (1992). "Local trends" are observed in suites of spatially and temporally associated MORB suites. These are interpreted to result from fractional crystallization.

# Fractional crystallization



Grove et al. (1992)



adapted from Langmuir et al. (1992)

TABLE 4. Comparison of Different Model "Inversions" of MORB Compositions for Melting Parameters

	$F_m$ , wt. %	$P_m$ , kbar	$P_o$ , kbar	$T_i$ , °C	CRUST, km
Mid Cayman Rise					
<i>Kinzler and Grove [1992a,b]<sup>a</sup></i>	7.7	8	12	1268	2.3
<i>Niu and Batiza [1991]<sup>b</sup></i>	13	6	8	1261	1.0
<i>Langmuir et al. [1992]<sup>c</sup></i>	7	9	13	1330	3
Reykjanes Peninsula					
<i>Kinzler and Grove [1992a,b]</i>	16	13	22	1435	10
<i>Niu and Batiza [1991]</i>	21	19	24	1429	7
<i>Langmuir et al. [1992]</i>	14	22	31	1550	13

<sup>a</sup>  $F_m$ ,  $P_m$ ,  $T_i$ , and CRUST were calculated with equations (1) - (4) in text,  $P_o$  was calculated with the equation  $P_o = 2 * P_m - P_f$ , where  $P_f$  is 4 kbar, as discussed in the text.

<sup>b</sup>  $F_m$  and  $P_m$  were calculated with equations (8)-(10) from *Niu and Batiza [1991]*,  $T_i$  was calculated with equation (8) and the solidus from Figure 4b from *Niu and Batiza [1991]*, and CRUST was calculated assuming passive upwelling with equation (4) presented in this study, using the estimated  $P_o$ ,  $P_f$  and  $F$  values from *Niu and Batiza [1991]*.

<sup>c</sup>  $P_o$  was calculated using equation (29) of *Langmuir et al. [1992]*,  $P_f$  was calculated based on the crustal thickness as determined with Figure 54,  $F_m$  was calculated based on  $P_o$ ,  $P_f$ , the melting function (1.05%/kbar), and the relationship  $F_m = F_{max}/2$ , and  $T_i$  was estimated with equation (29) and the solidus relationship of *Langmuir et al. [1992]*.



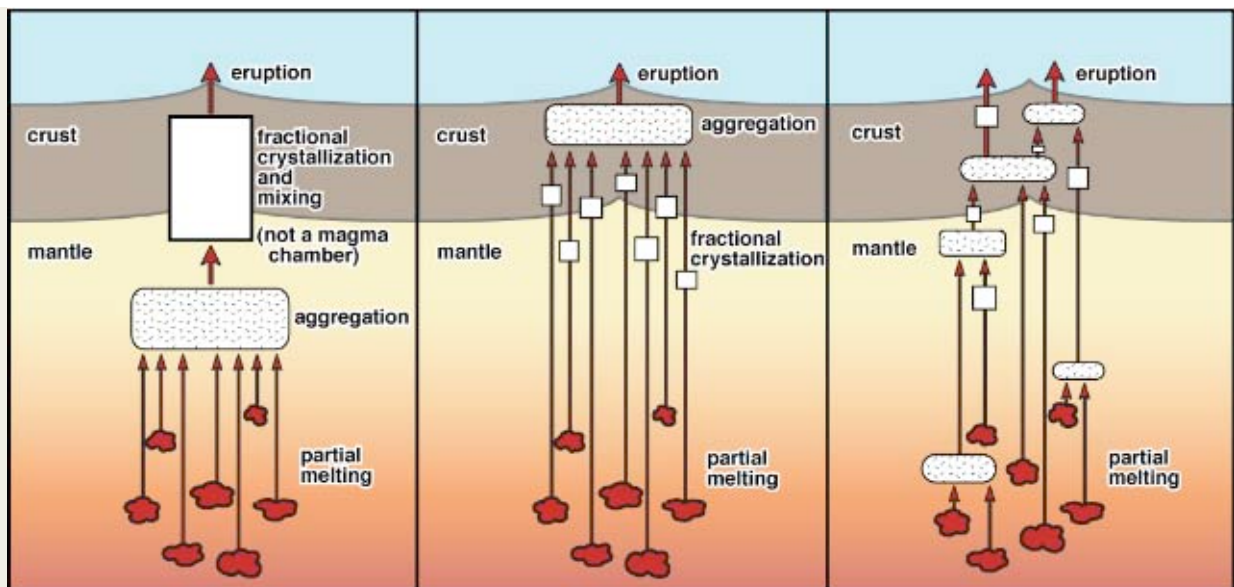
Field work on the East Pacific Rise 10 – 12° N.

What we know of the mid-ocean ridge magmatic system comes from:

Direct sampling of lavas  
By ALVIN, ROV's (remotely operated vehicles, e.g. JASON)

Gravity measurements from ships on the surface

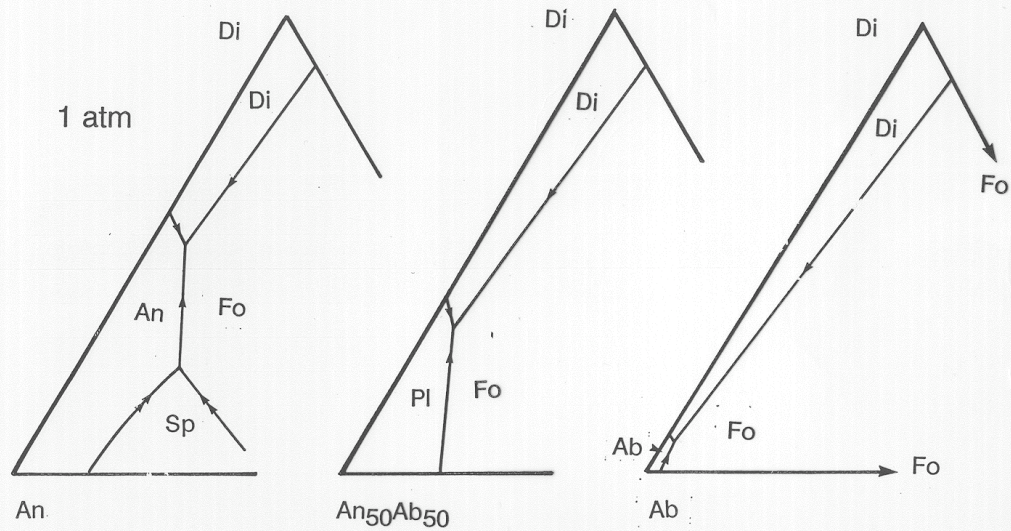
OBS (Ocean Bottom Seismometers) MELTS experiment



Decades of discussion and debate exist on the nature of mantle melting, fractional crystallization and magma mixing processes in the MORB environment. Here are some possibilities.

As we shall see, there is strong evidence in the petrology of MORB lavas that supports some variant of model #3. The key evidence is preserved in the minerals & chemistry of MORB lavas.

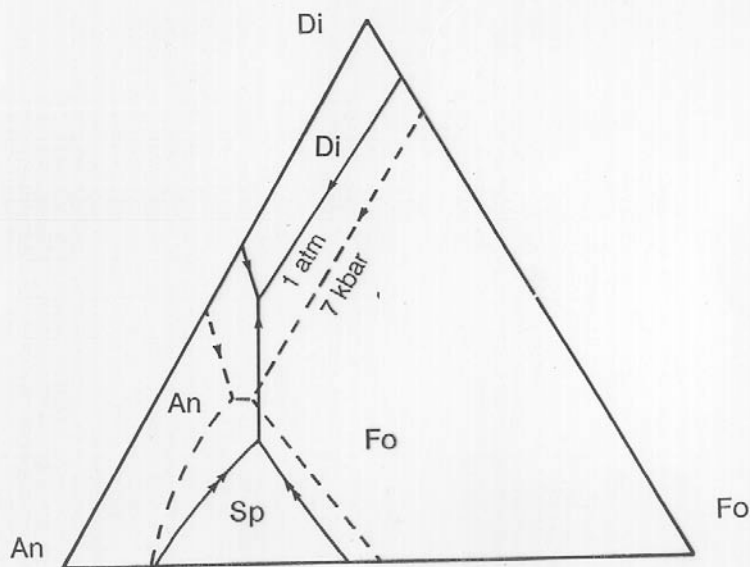
Grove et al. (1992)



Systematic behavior of the phase boundaries in “simple” basalt analog systems inspire phase diagram-based models of the phase relations for MORB crystallization.

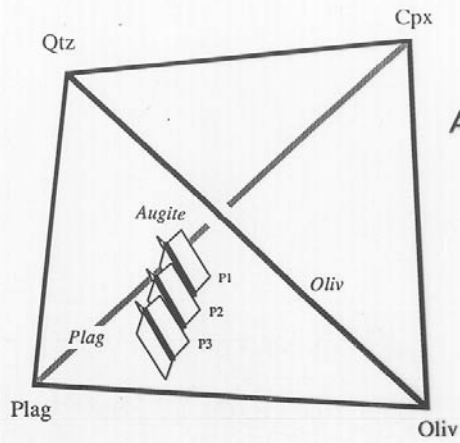
Here in the system Forsterite – Diopside – Plagioclase note what happens to the Fo- Di – Plag piercing point (the gabbro cotectic) as the An content of the plagioclase changes.

Grove et al. (1992)

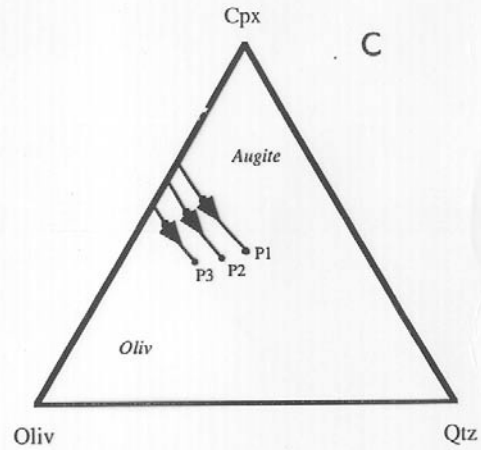
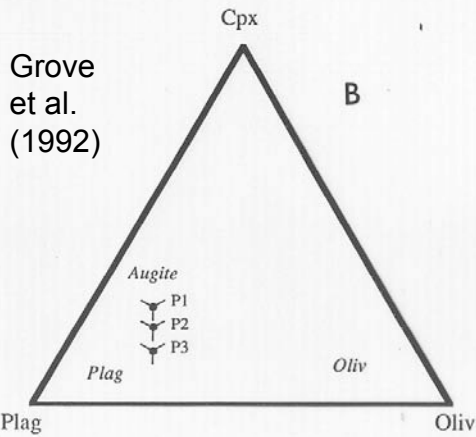


This diagram shows the phase boundary shifts in Forsterite – Diopside – Anorthite from 1 atm to 700 MPa. The key observation here is the the Forsterite – Anorthite boundary does not move over the pressure range of 0.1 MPa to 500 MPa.

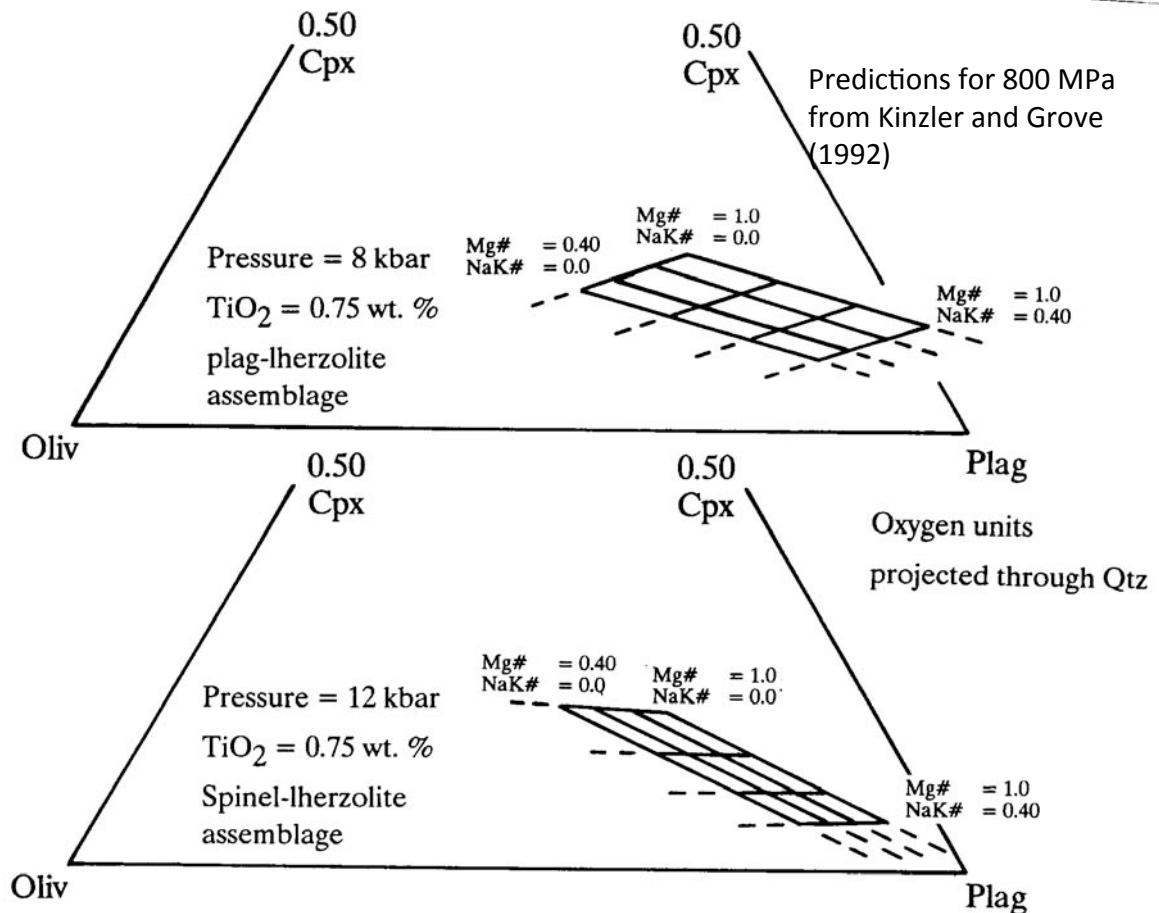
Grove et al. (1992)



P1, P2 and P3 = Oliv + Opx + Cpx + Plagioclase multiple saturation points: we can predict these from experimental data.



We can use these observations to develop a model for predicting the phase boundaries for MORB crystallization over the pressure range expected in the oceanic lithosphere: 0.1 MPa to 500 MPa.



# Piston Cylinder



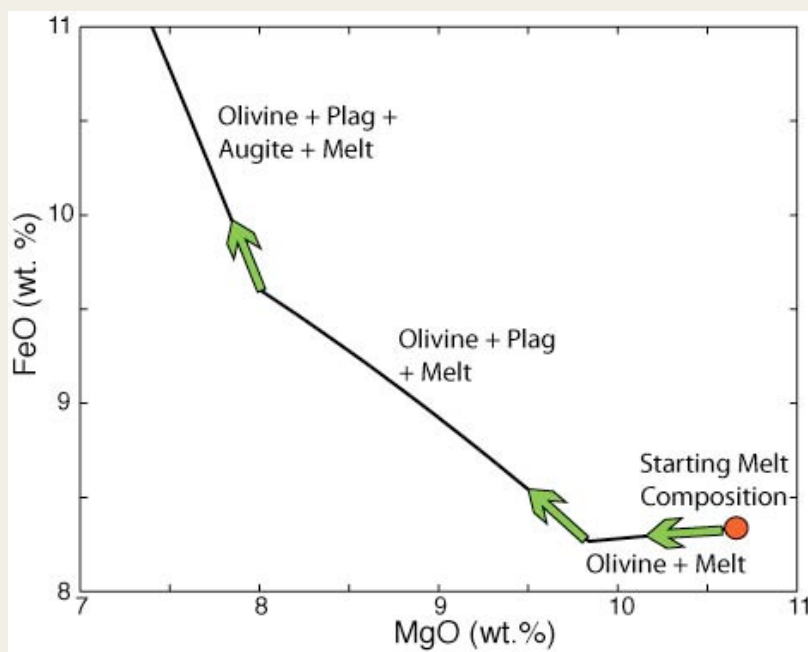
Crystallization models are calibrated by direct experimental determination of liquids saturated with the appropriate phase assemblages:

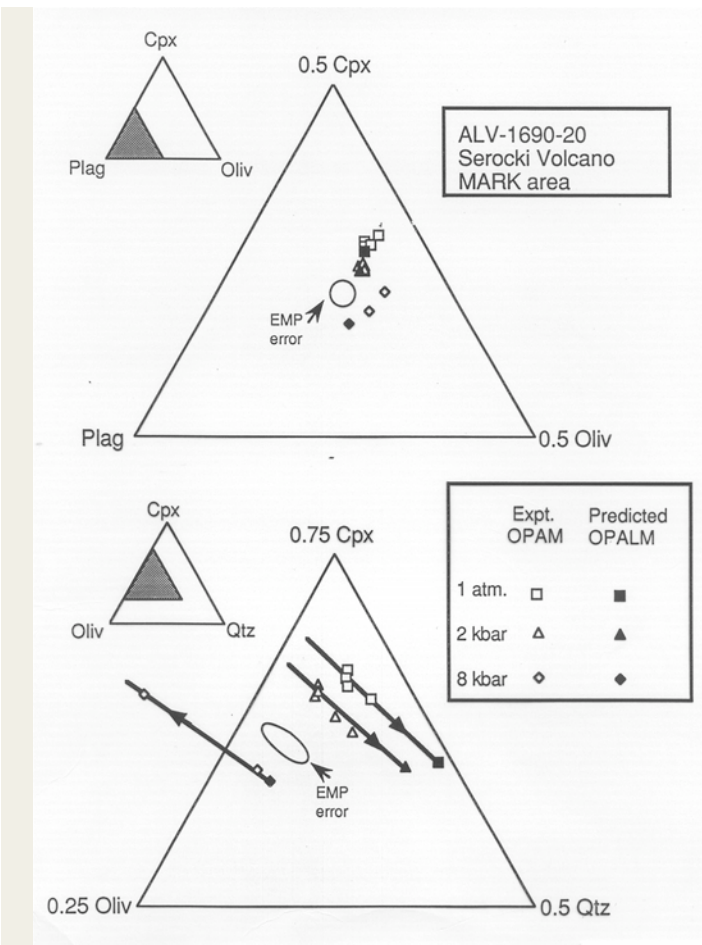
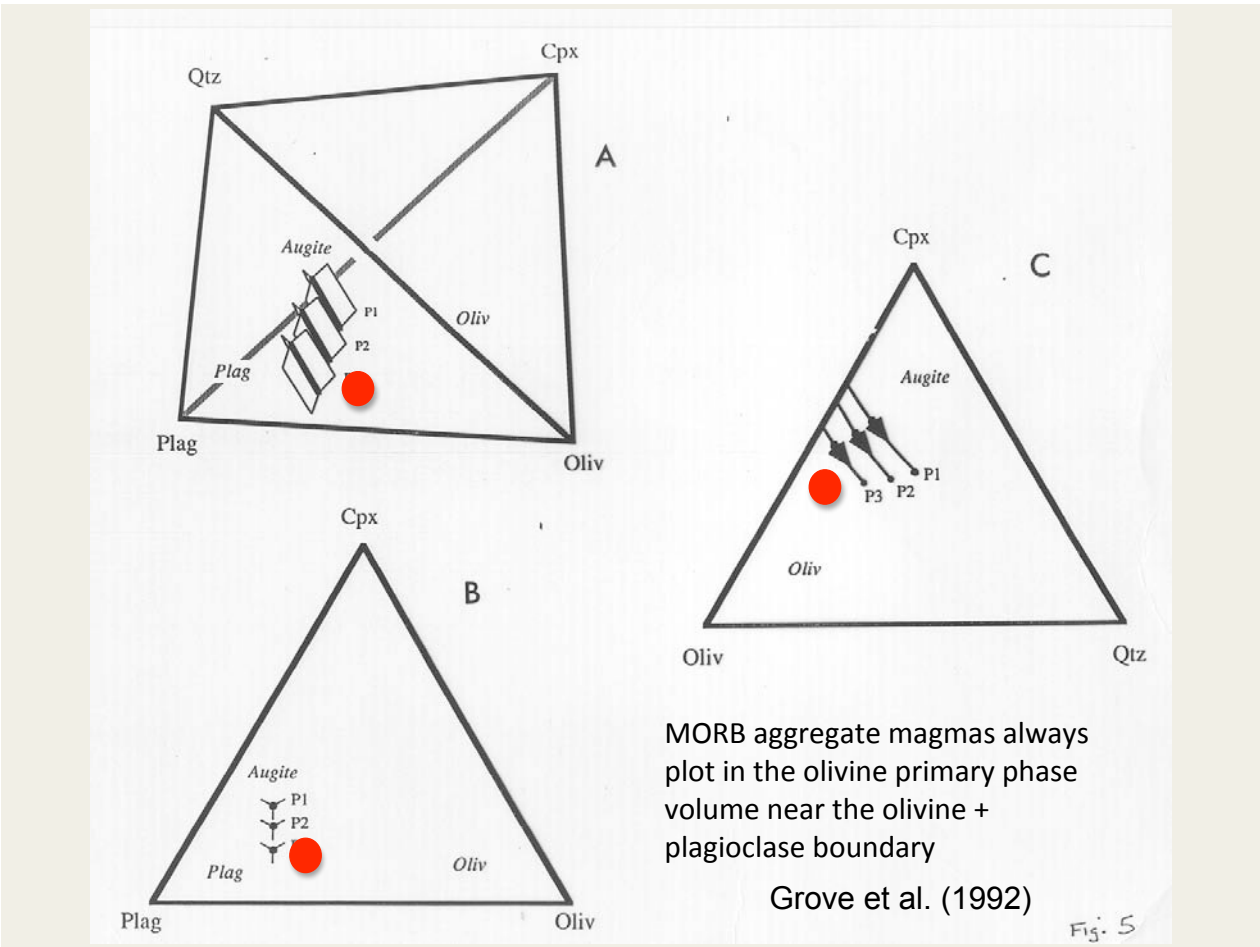
Olivine

Olivine + Plagioclase

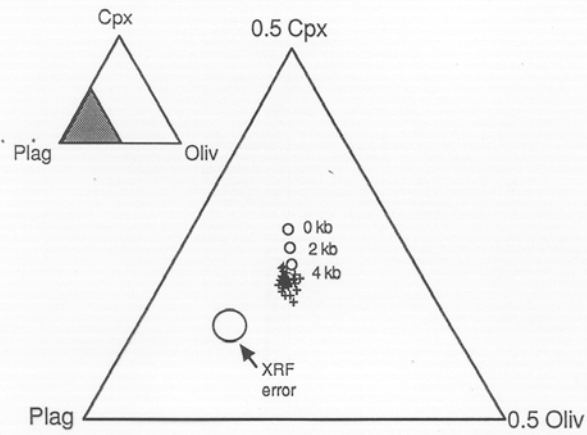
Oliv +  
Clinopyroxene +  
Plagioclase

Liquid line of descent (LLD) for MORB will follow this path

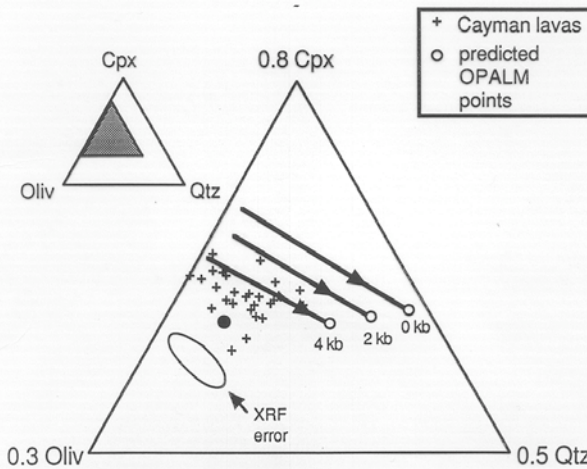




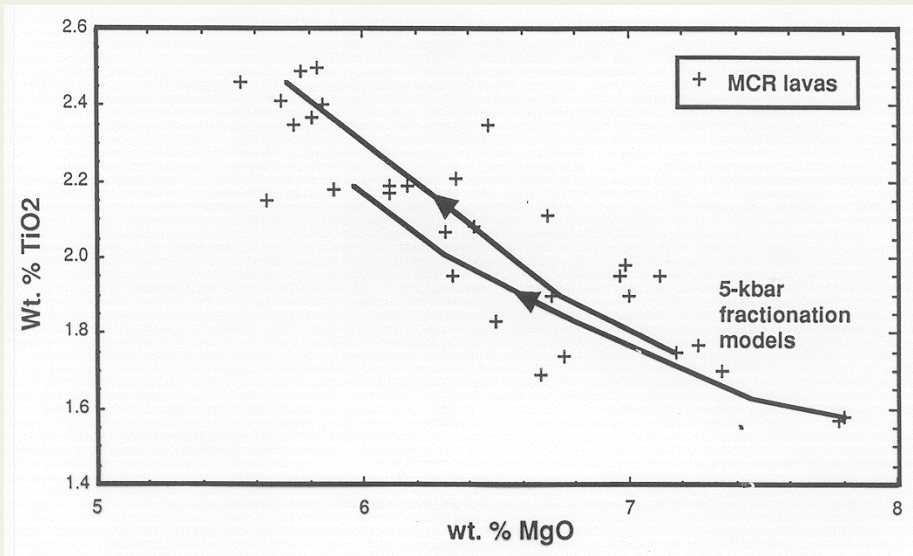
This set of projections shows how well our fractional crystallization model predicts the olivine + plagioclase + clinopyroxene + liquid (OPAM) saturation boundary for a set of experiments that contain such liquid + crystal assemblages from 0.1 to 800 MPa.



When spatially and temporally associated MORB lava suites are plotted in these projection schemes with predicted phase boundaries there are systematics that relate to the spreading rate of the ridge segment – slower spreading = deeper fractional crystallization.

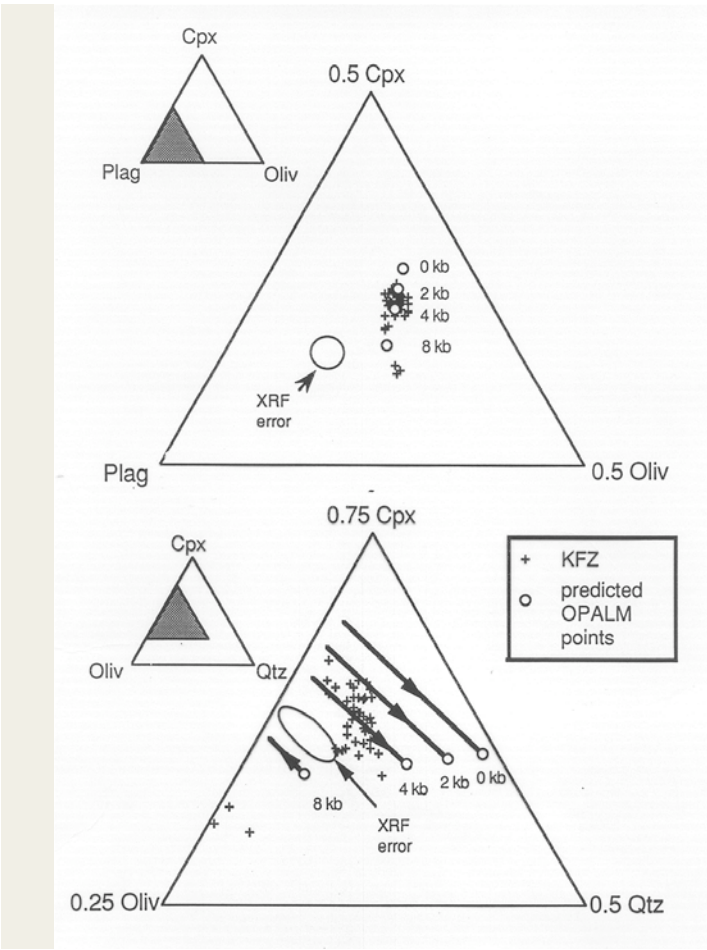


Grove et al. (1992)



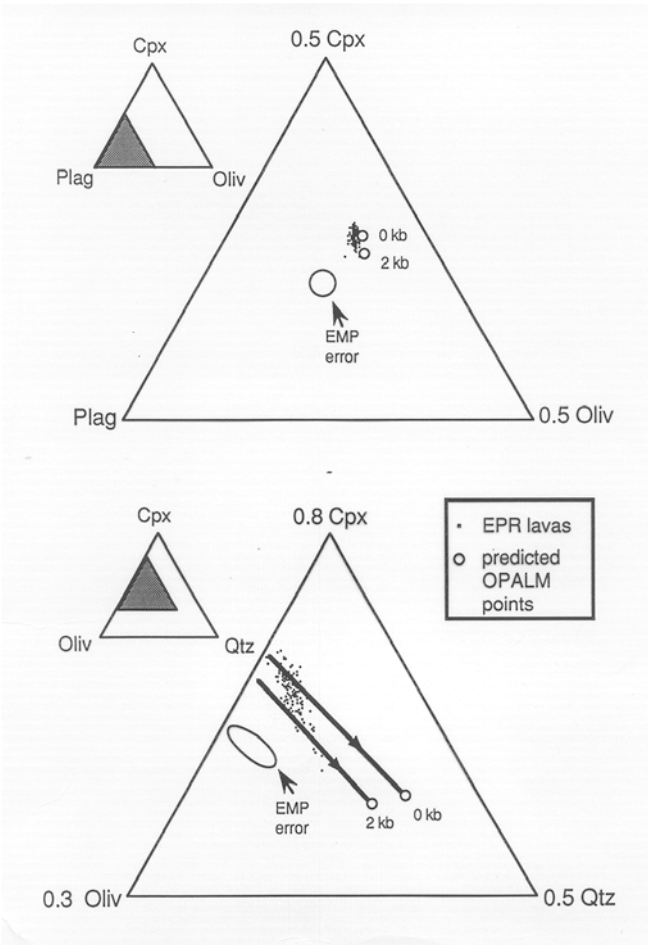
It is important to track minor elements in this process. In the case of the Cayman lavas, we predict that high-Ca clinopyroxene will crystallize early at elevated pressures. TiO<sub>2</sub> abundance variations will be very sensitive to early Cpx crystallization. Note the steep slopes for Oliv + Plag + Cpx which match the natural lavas.

Grove et al. (1992)



Another ridge segment (the Kane Fracture Zone (KFZ) on the mid-Atlantic Ridge where elevated pressure fractional crystallization has occurred.

Grove et al. (1992)



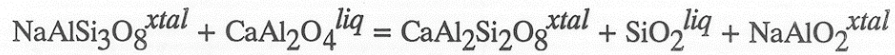
At fast spreading environments we find no evidence for elevated pressures of fractional crystallization.

This is consistent with seismic observations from OBS deployments that have detected magma lenses at shallow depths beneath the sea floor (1 to 3 km).

Grove et al. (1992)

Another important characteristic to track in MORB systems is the effect of pressure, temperature and magma composition on the composition of plagioclase that crystallizes from a melt.

Plagioclase - liquid equilibria treated using the exchange reaction:



$$K_D^{Ca-Na} = \frac{[X_{An}^{xtal}][X_{SiO_2}^{liq}][X_{NaAlO_2}^{liq}]}{\{[X_{Ab}^{xtal}][X_{CaAl_2O_4}^{liq}]\}}$$

Data set = 171 assemblages. Pressure range = 0.001 to 27 kbar.

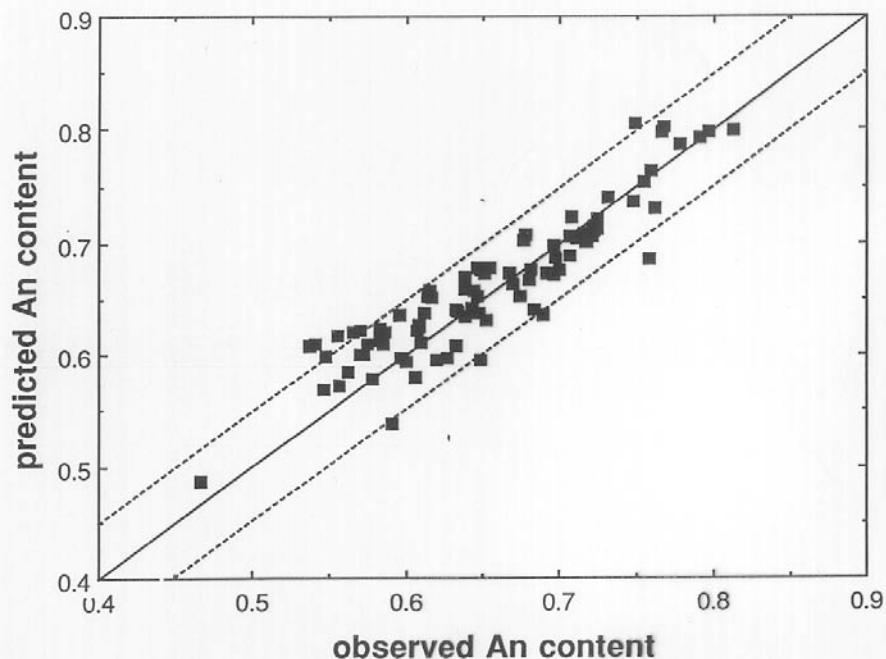
Plagioclase components are mole fraction An, Ab and Or.

Liquid components from Bottinga and Weill (1972). Model  $R^2 = 0.88$ .

$$\text{Log } K_D^{Ca-Na} = 11.1068 - 0.0338 * P \text{ (in kbars)} - 4.4719 * (1 - X_{NaAlO_2}^{liq})^2 - 6.9707 * (1 - X_{KAlO_2}^{liq})^2$$

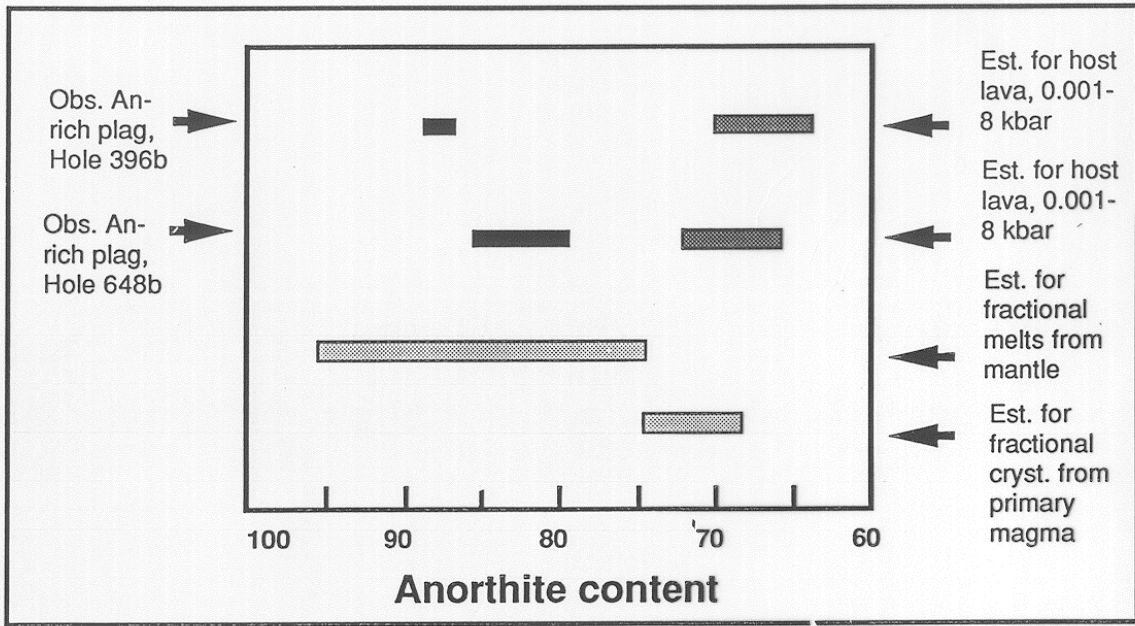
One can solve explicitly for plagioclase An content.

Grove et al. (1992)



We can recover the experimental observations to within 5 An units with our model which depends only on pressure and magma composition.

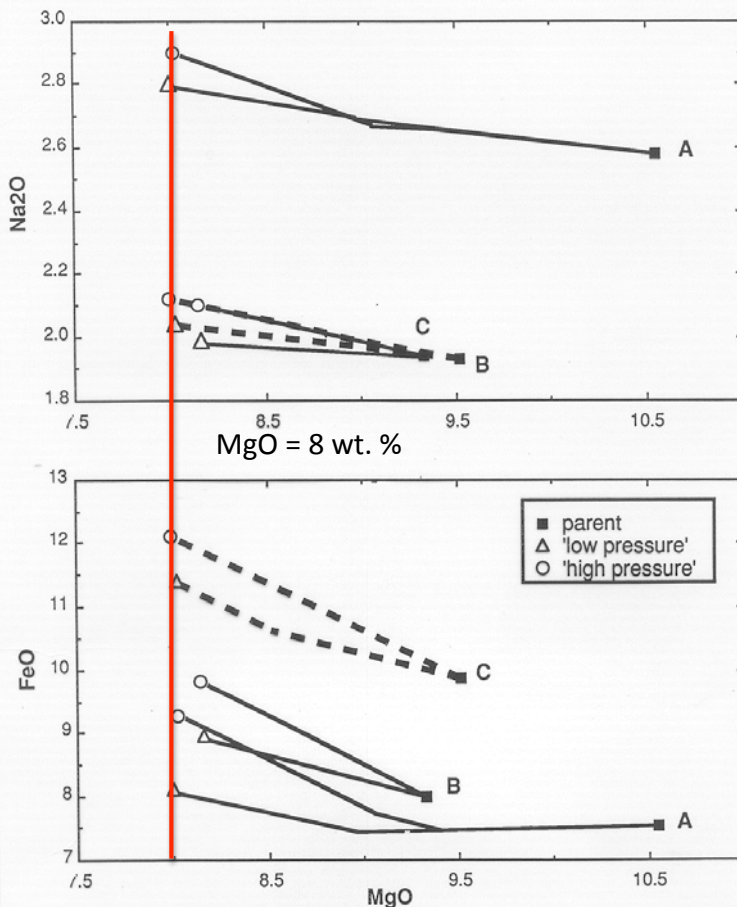
Grove et al. (1992)



Grove et al. (1992)

When we examine the compositions of plagioclase found in MORB lavas from a variety of MORB suites they reveal an additional complexity that allows us to understand the complexity that we need to infer to explain MORB lava compositional variability.

Hole 396B was drilled by ODP in young oceanic crust near the Kane Fracture Zone.

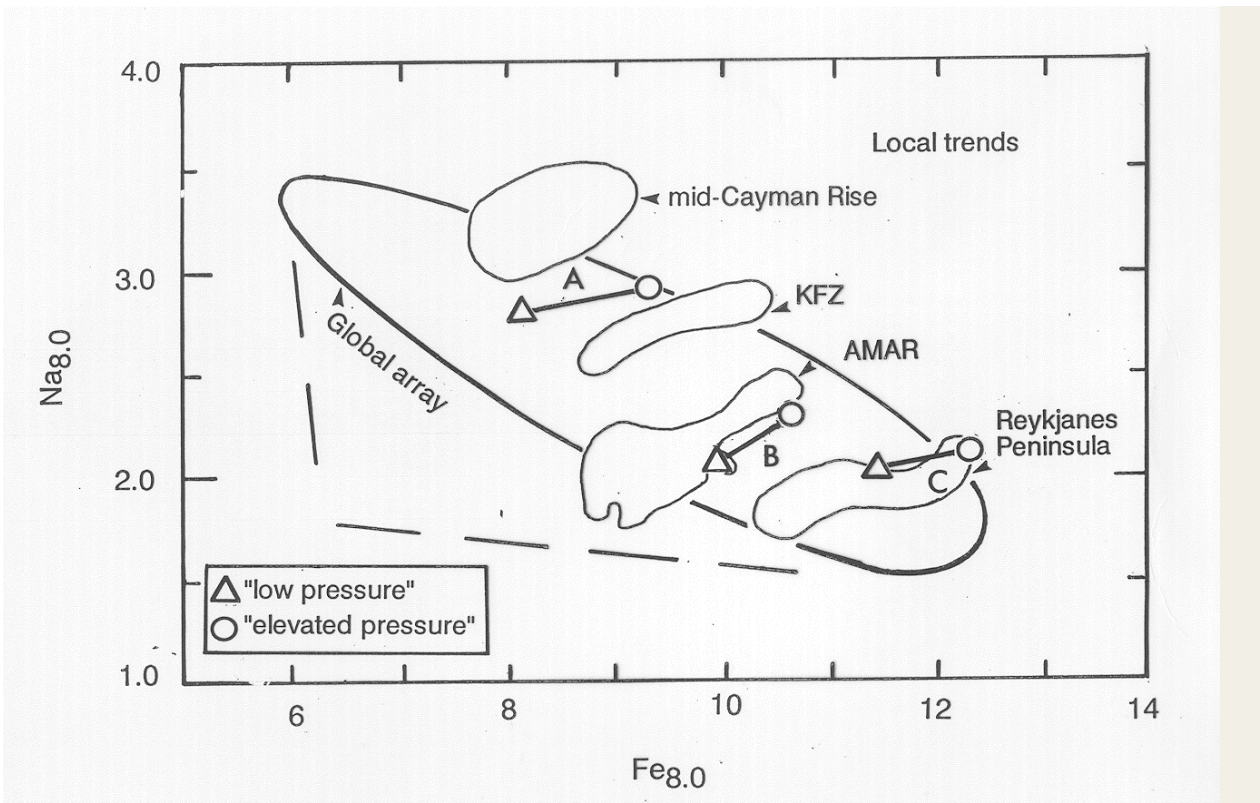


A, B and C are pooled near-fractional melts from 3 different  $T_p$ 's.

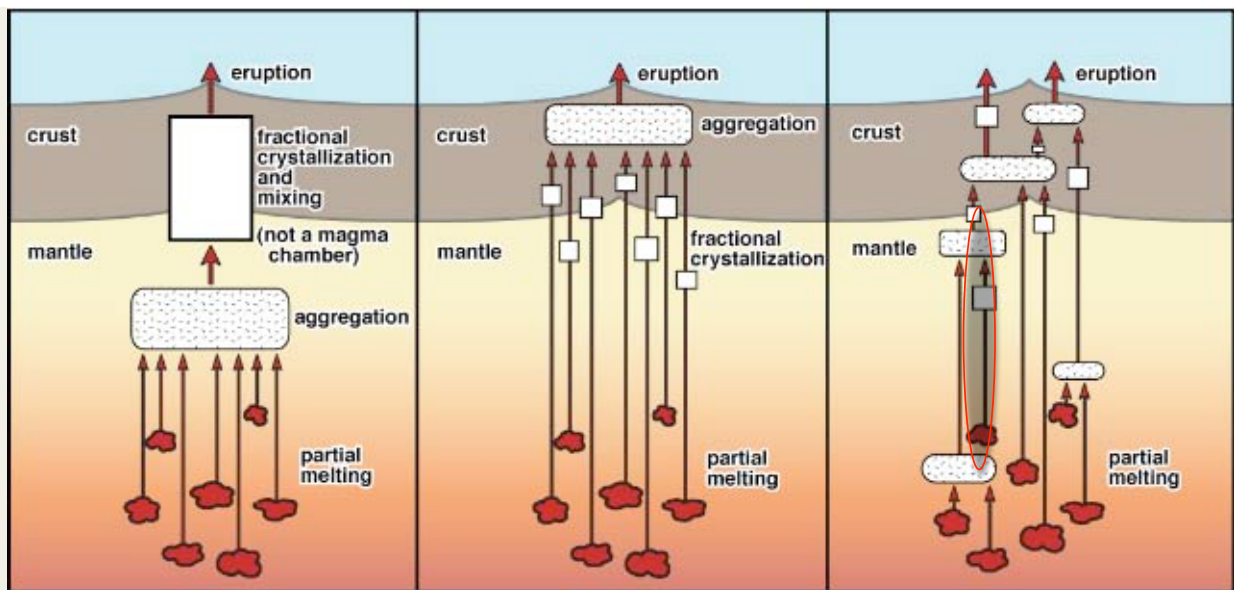
These variation diagrams show Na<sub>2</sub>O and FeO plotted against MgO, and the tow paths represent fractional crystallization (F.C.) processes imposed at different pressures. The depth (pressure) of F.C. depths on the thermal structure of the oceanic lithosphere.

Lithosphere Temperature is imposed by spreading rate and hydrothermal cooling.

Grove et al. (1992)



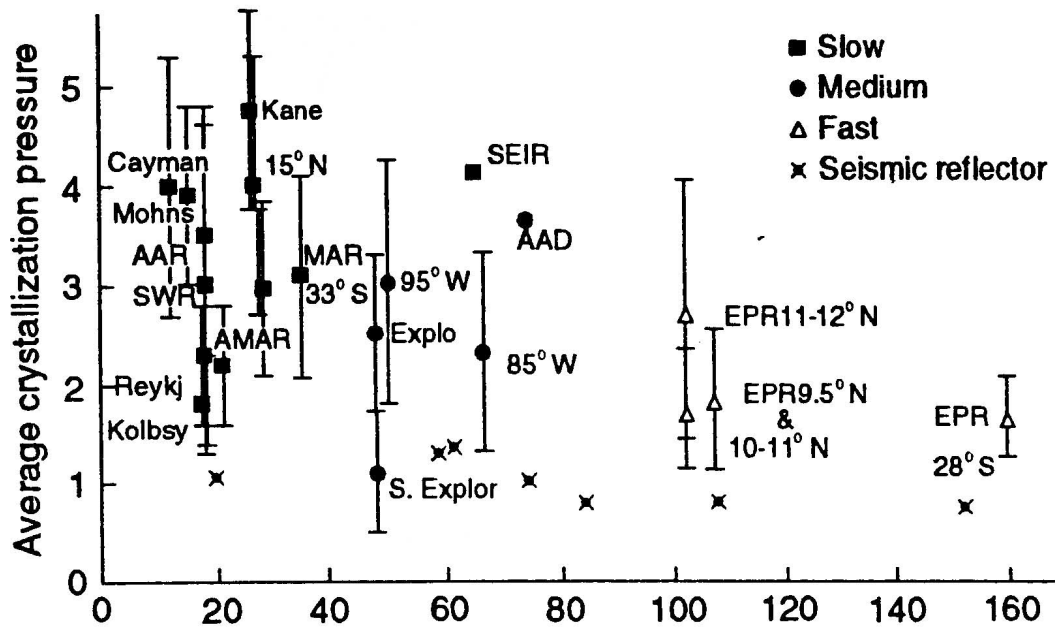
Melting models plotted on  $Na_8$  vs.  $Fe_8$  projection of Langmuir et al. (1992). "Local trends" are observed in suites of spatially and temporally associated MORB suites. These are interpreted to result from fractional crystallization at a range of pressures.



After Grove et al. (1992)

Decades of discussion and debate exist on the nature of mantle melting, fractional crystallization and magma mixing processes in the MORB environment. Here are some possibilities.

Evidence preserved in the plagioclase of MORB lavas that supports some variant of model #3. The evidence points to crystallization of a depleted mantle melt prior to mixing in a near surface magma chamber.



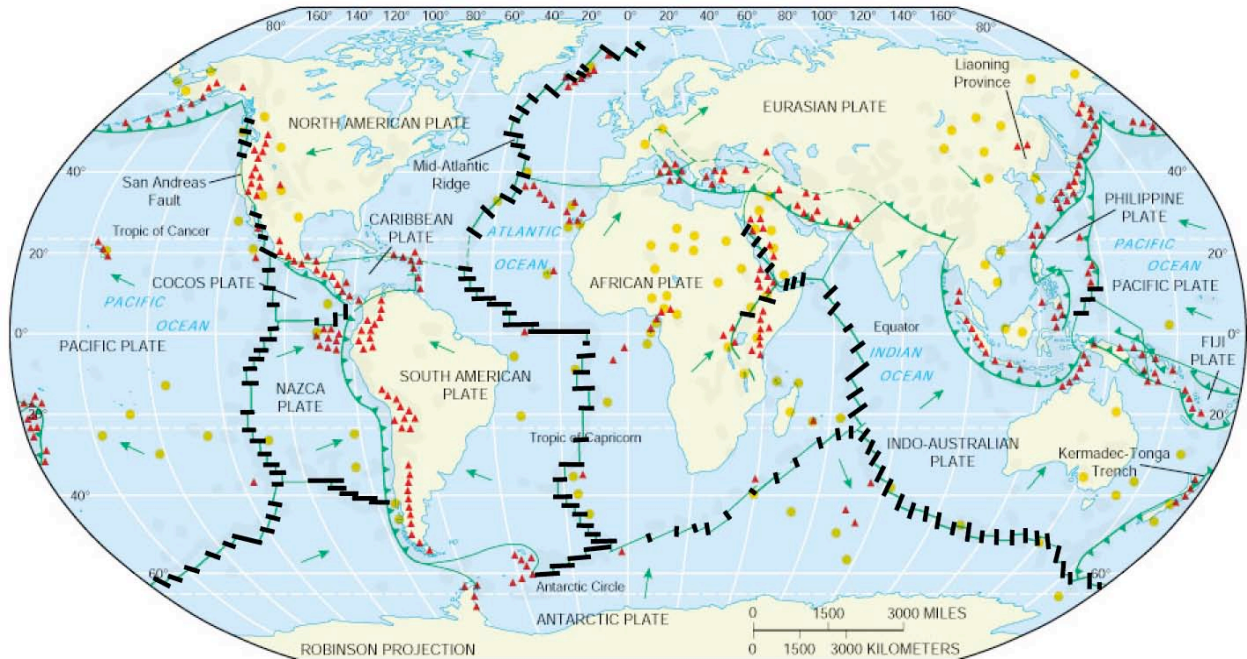
From Grove (2000)

Here we show estimates of the maximum pressure of fractional crystallization vs. half spreading rate. Note that slower spreading is correlated with higher pressure of fractional crystallization.

We'll see how this observation is reinforced when thermal models of oceanic lithosphere are coupled with melting and crystallization.

# Global distribution of oceanic transform faults

## 120+ transform fault systems



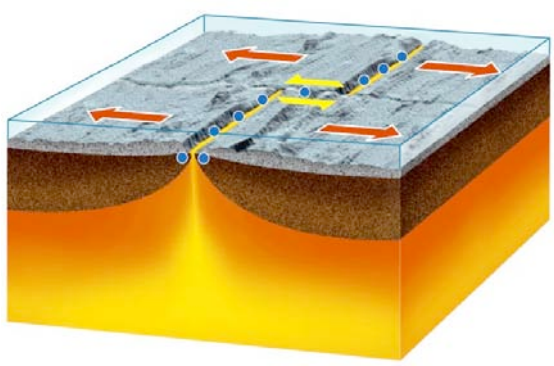
- ▲ volcanoes
- hot spots
- oceanic transform fault
- divergent boundary
- ▼ convergent boundary
- motion vector

<http://www.usgs.gov>

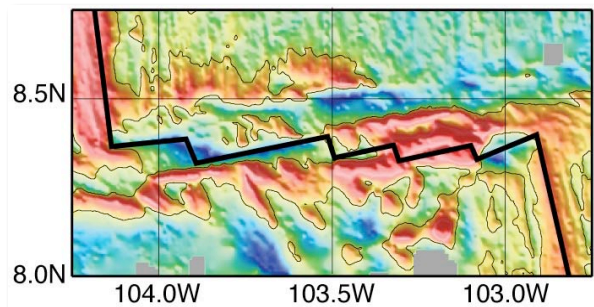
## Conclusions

**Segmentation of oceanic transform faults is VERY important.**

- Fault structure
- Mantle flow and melt extraction



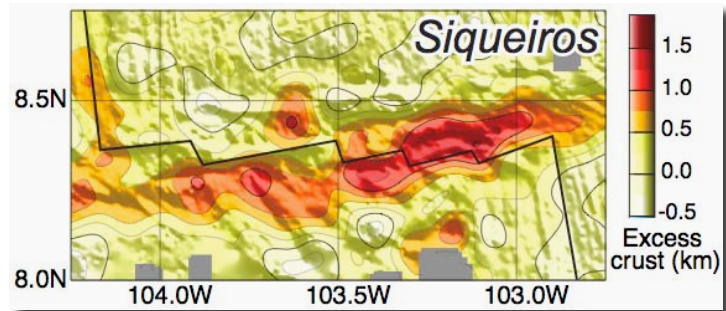
Textbook transform fault:  
Single fault strand!



Natural transform fault:  
Segmented!

### Motivation:

Gravity calculations at fast-slipping transform faults suggest the possibility of crustal thickening within the transform fault domain.



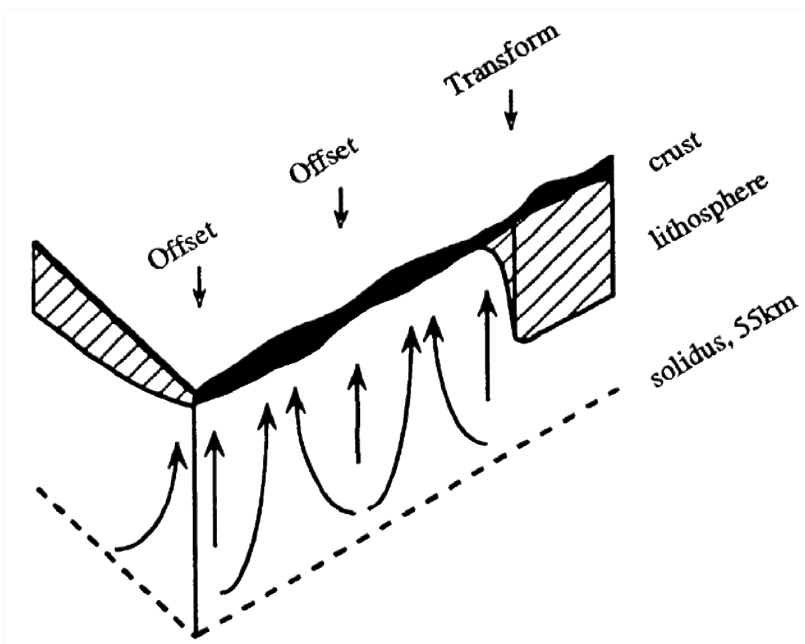
Gregg et al., *Nature* (2007)

### Questions:

- How does fault segmentation effect mantle flow, melt generation, and melt extraction at a transform fault?
- Could segmentation lead to thicker crust within fast-slipping transform faults?

### Approach:

We use coupled 3D thermal and melting models of segmented transforms to investigate the sensitivity of crustal production and lava composition to melt migration.



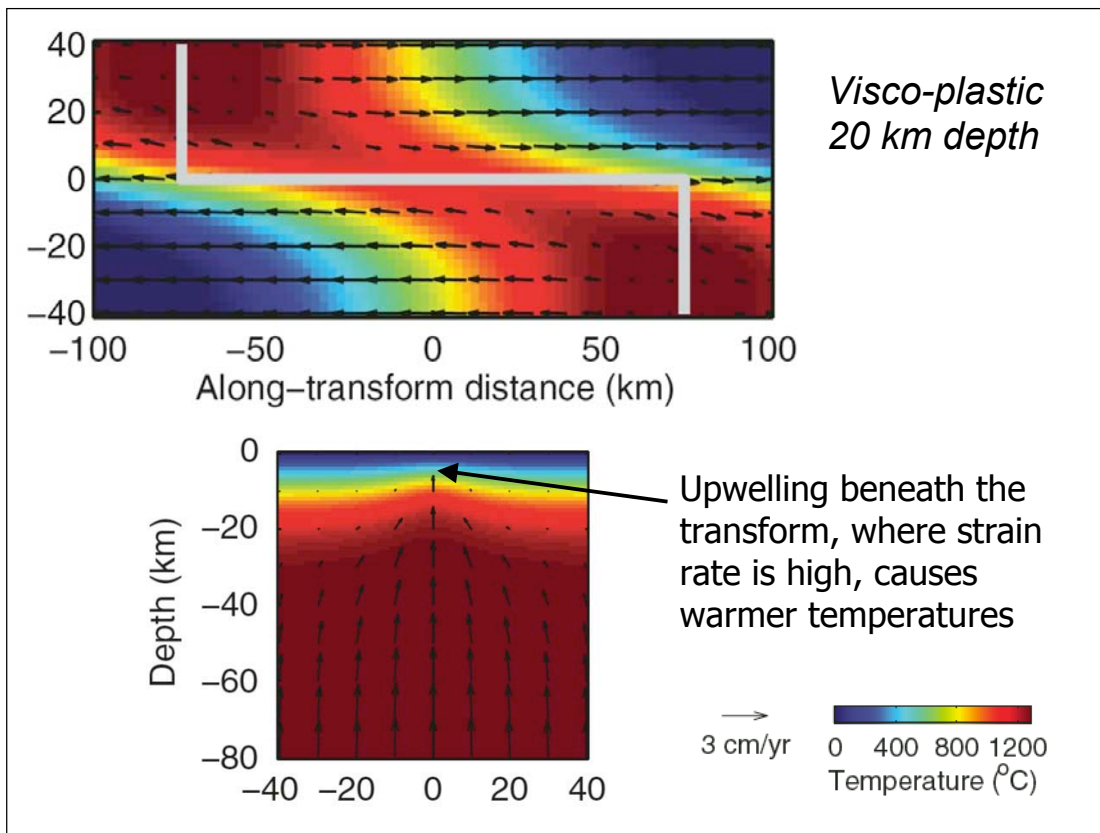
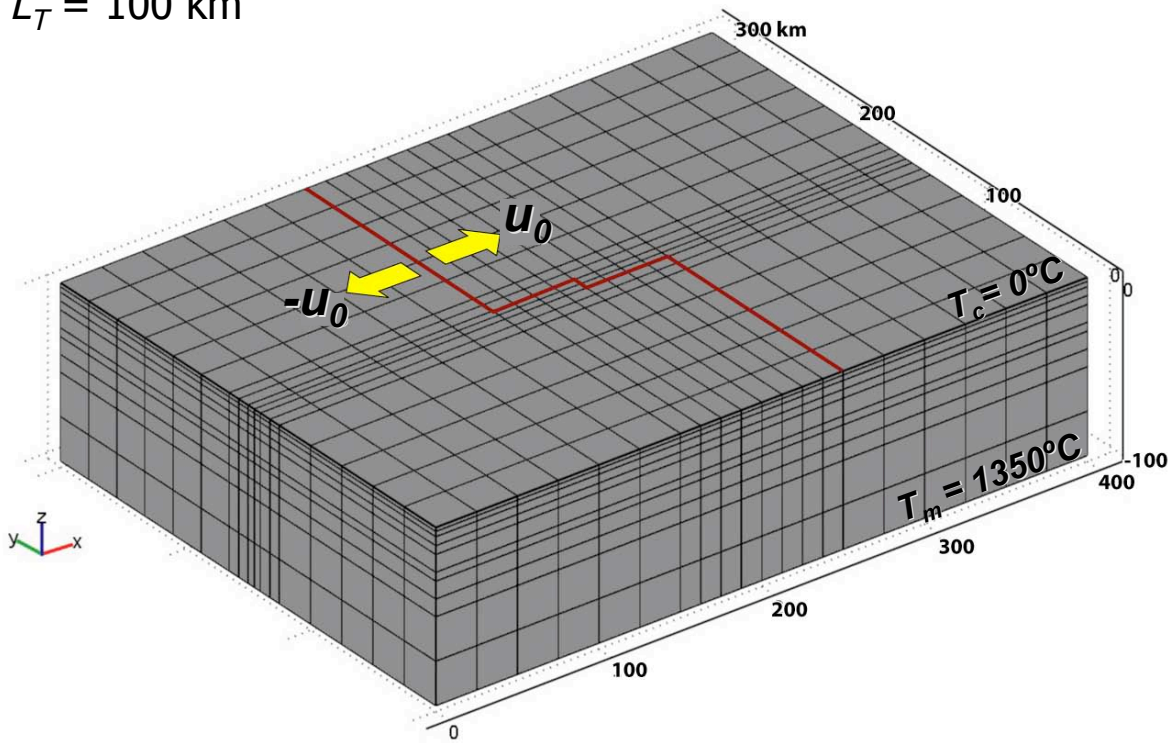
The geochemical transform fault effect: Deep, low extents of melting

How can we produce thick crust within the transform fault, AND reproduce the observed geochemical transform fault effect?

3D Generic model:

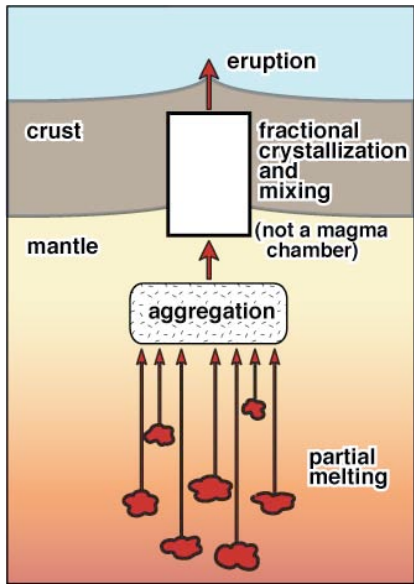
$$u_0 = 50 \text{ mm/yr}, L_{ITSC} = 10 \text{ km}$$

$$L_T = 100 \text{ km}$$

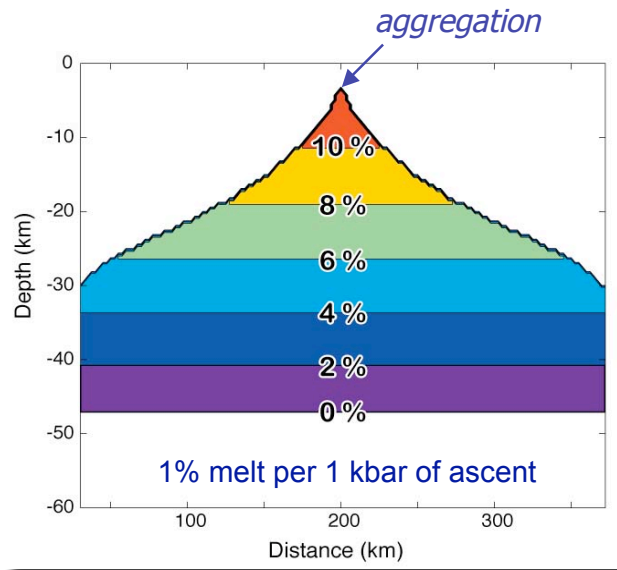


## Melt model calculations:

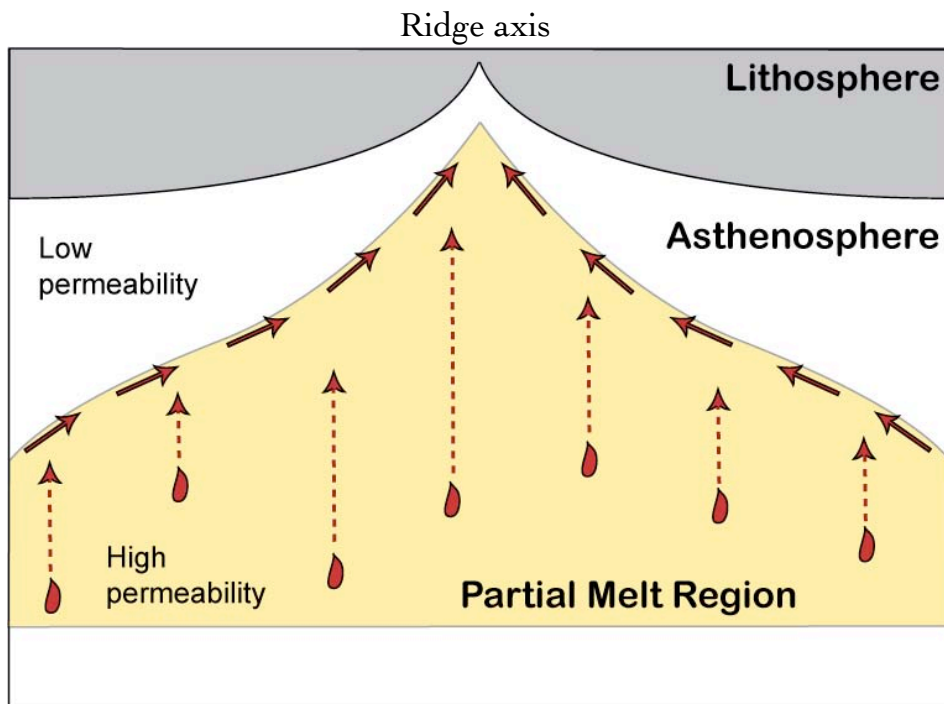
- (1) Near fractional melting, Kinzler & Grove (1992a,b, and 1993)
- (2) Pooling of melt (aggregation)
- (3) Fractional crystallization, Yang et al. (1996)



Grove et al. (1992)

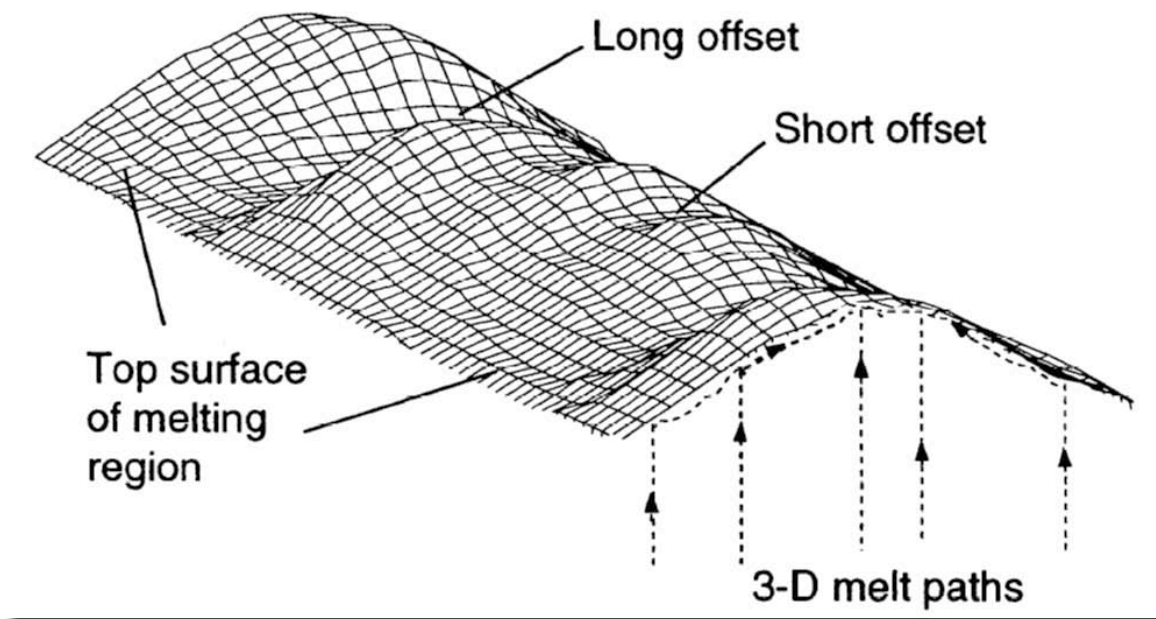


## Melt Migration



Adapted from Sparks and Parmentier, *EPSL* (1991)

# Melt Migration



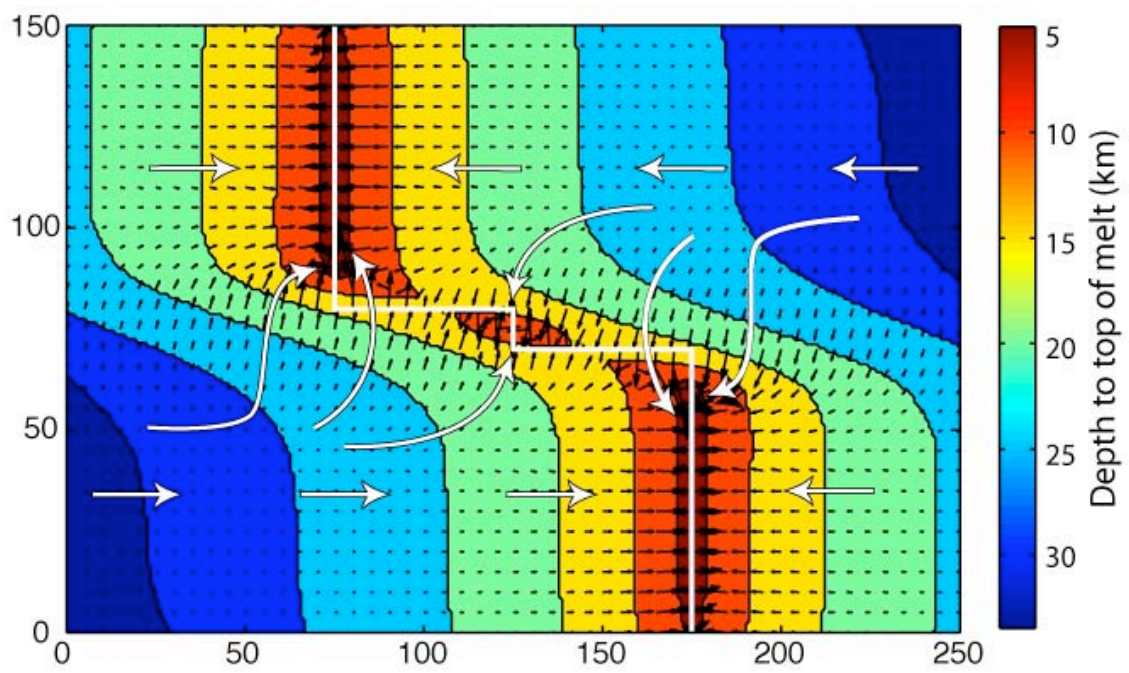
Magde and Sparks, *JGR* (1997)

## Melt pooling in 3D

Model parameters:

Visco-plastic rheology, Workman & Hart (2005) DMM composition

$Nu = 4$ ,  $T_p = 1350^\circ\text{C}$

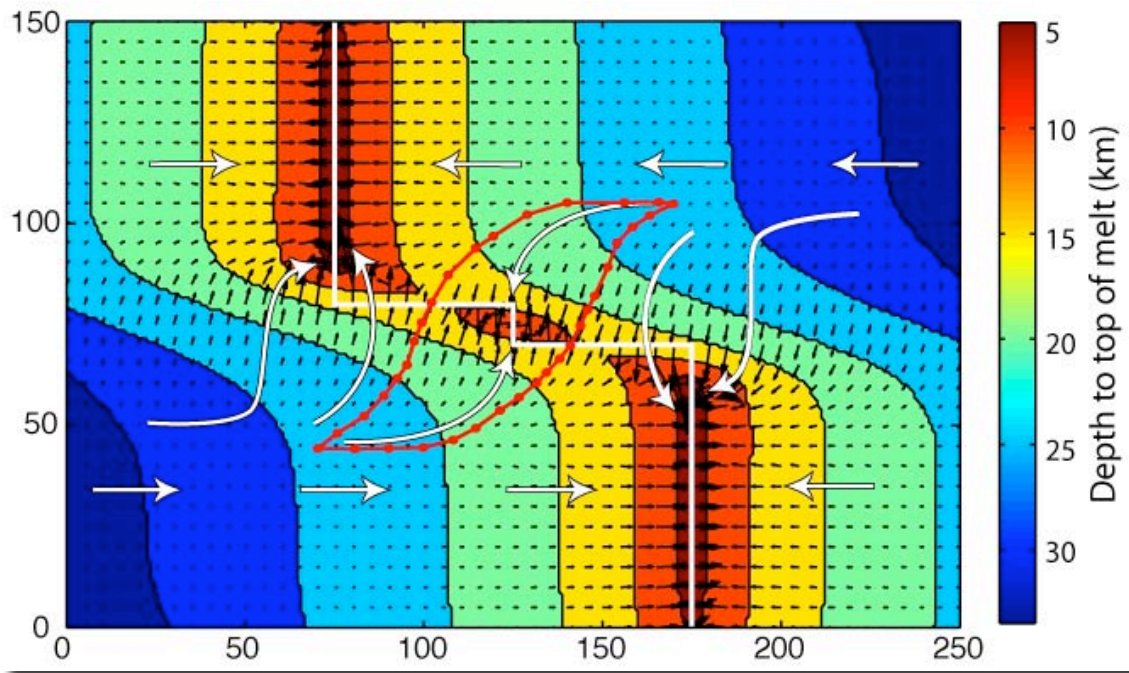


## Melt pooling in 3D

Model parameters:

Visco-plastic rheology, Workman & Hart (2005) DMM composition

$Nu = 4$ ,  $T_p = 1350^\circ\text{C}$

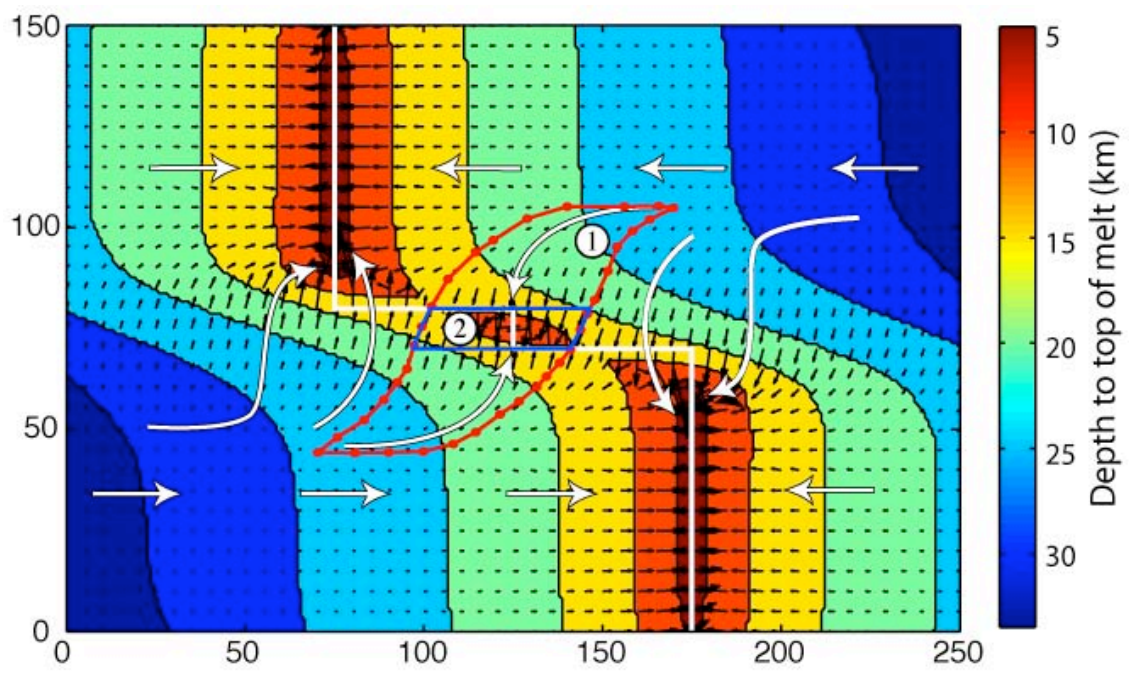


## Melt pooling in 3D

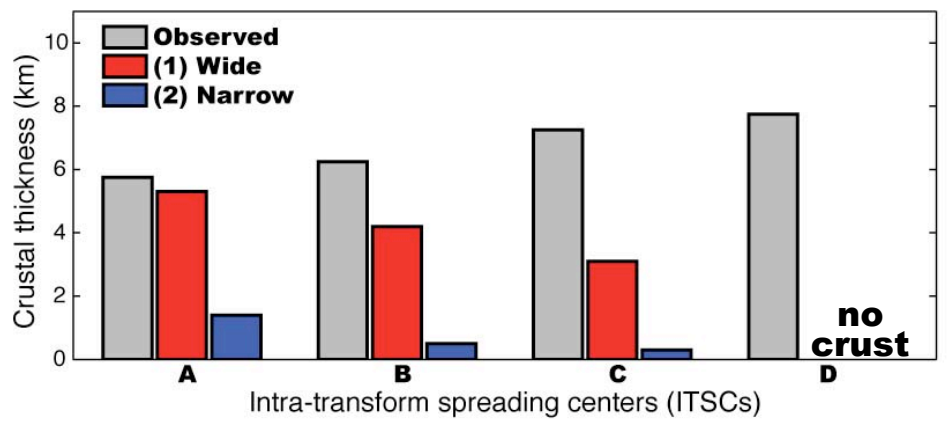
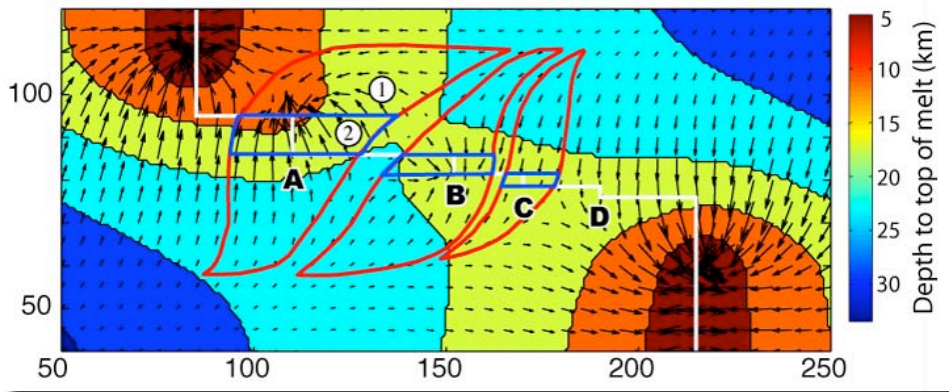
Model parameters:

Visco-plastic rheology, Workman & Hart (2005) DMM composition

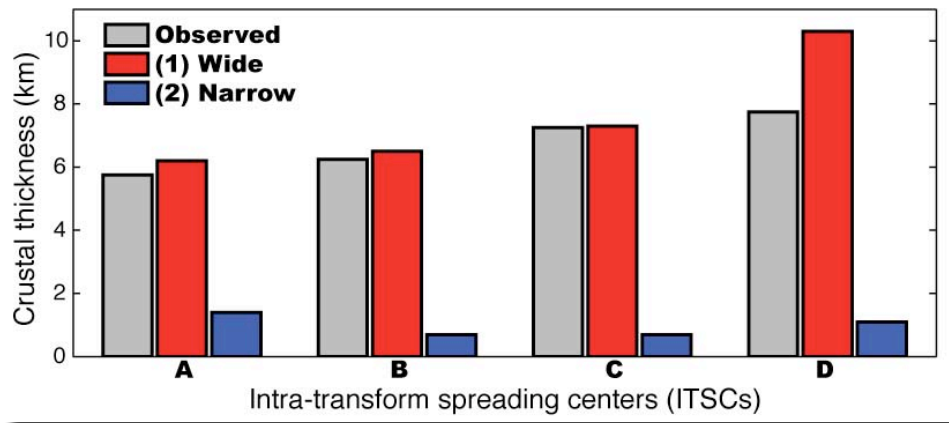
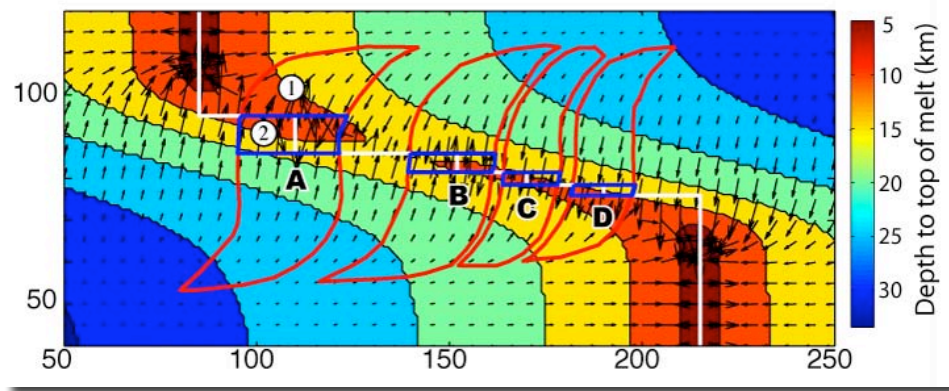
$Nu = 4$ ,  $T_p = 1350^\circ\text{C}$

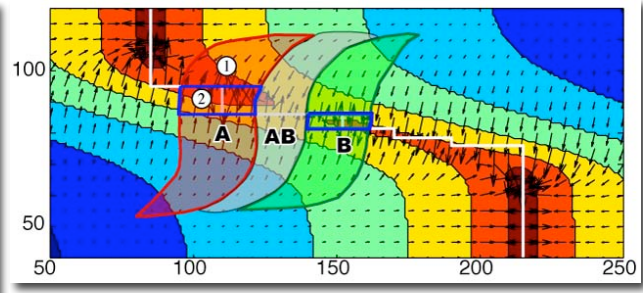
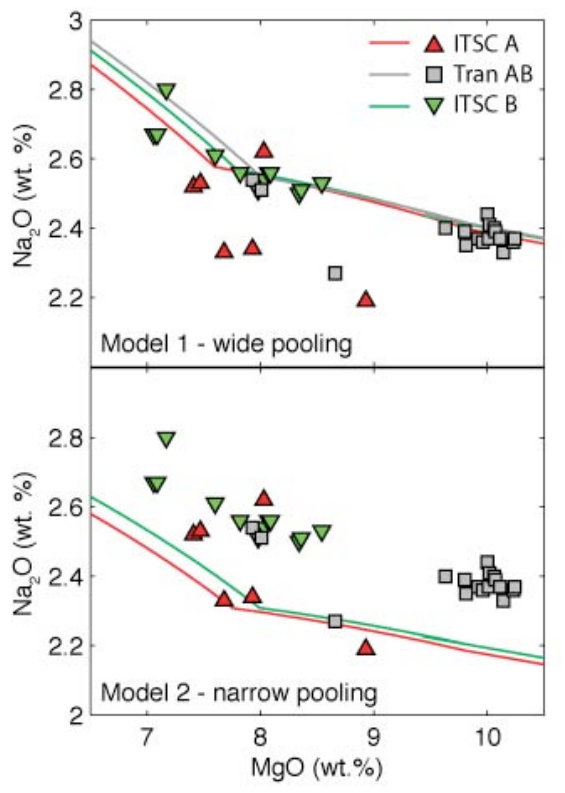


### Siqueiros - Constant viscosity



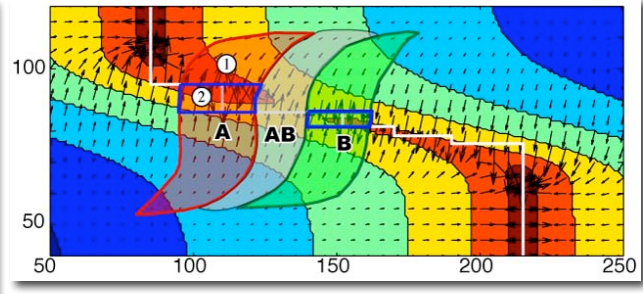
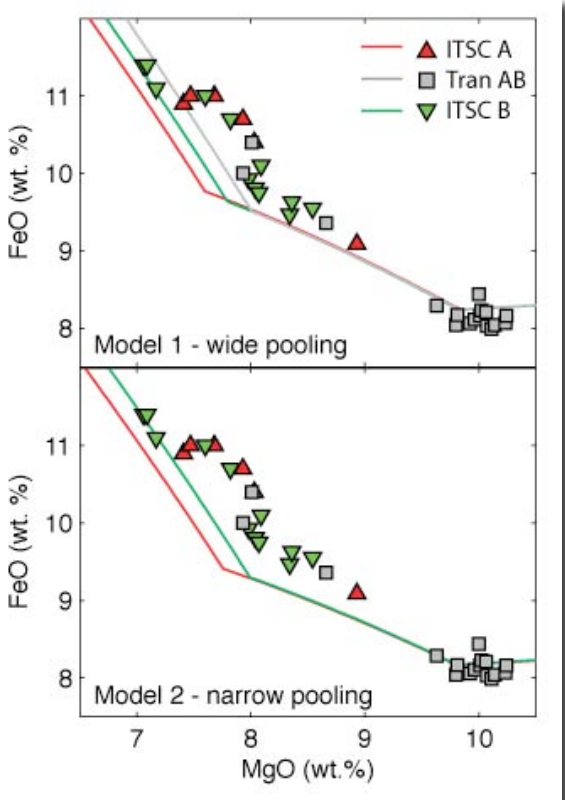
### Siqueiros - Visco-plastic viscosity





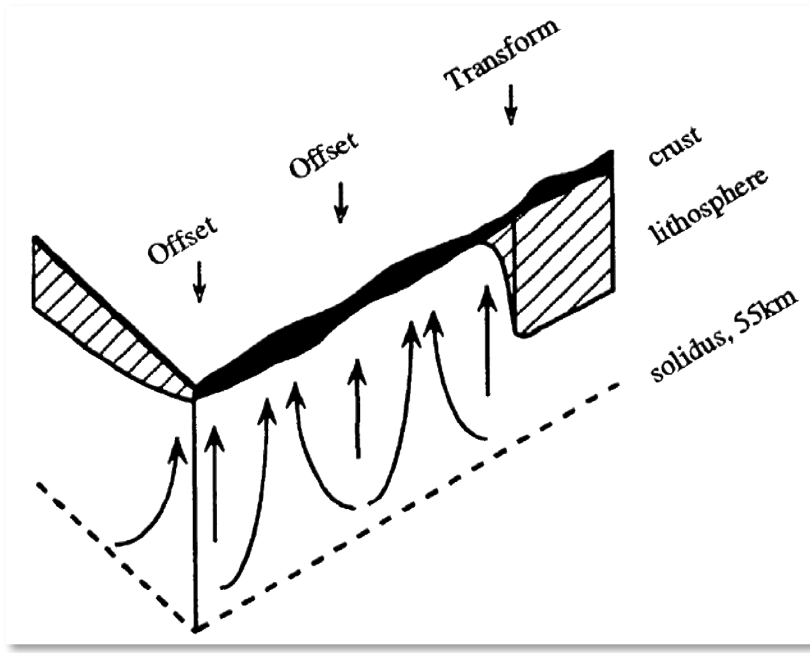
$T_p = 1350^\circ\text{C}$ ,  $Nu = 4$ , visco-plastic  $\eta$

Data from Perfit et al. (1996), Hays (2004)



$T_p = 1350^\circ\text{C}$ ,  $Nu = 4$ , visco-plastic  $\eta$

Data from Perfit et al. (1996), Hays (2004)



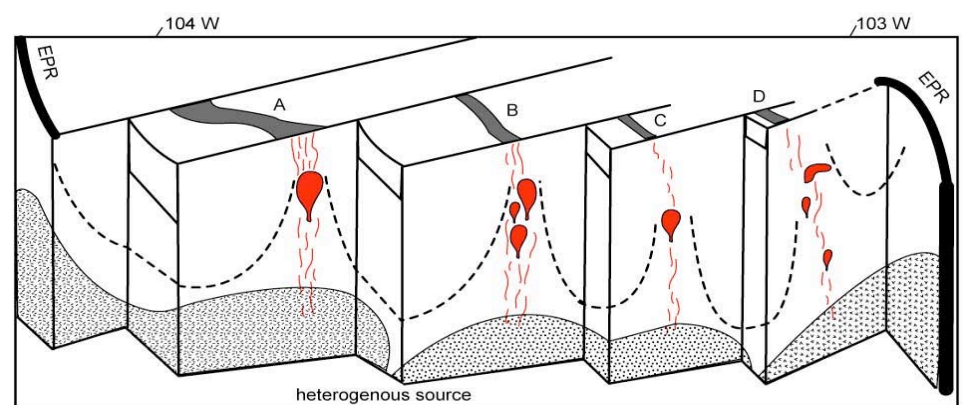
The geochemical transform fault effect: Deep, low extents of melting

How can we produce thick crust within the transform fault, AND reproduce the observed transform fault effect?

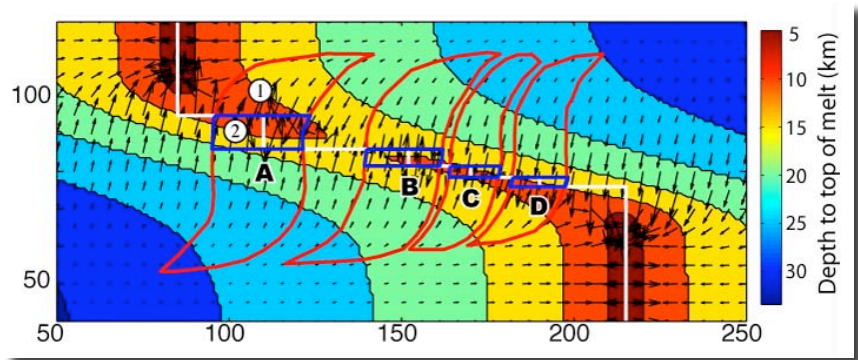
**WIDE POOLING!**

Reynolds & Langmuir (1997)

### The Siqueiros plumbing system...



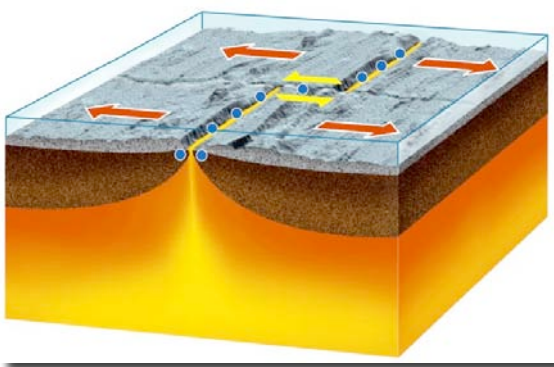
Based on Fornari et al., MGR (1989)



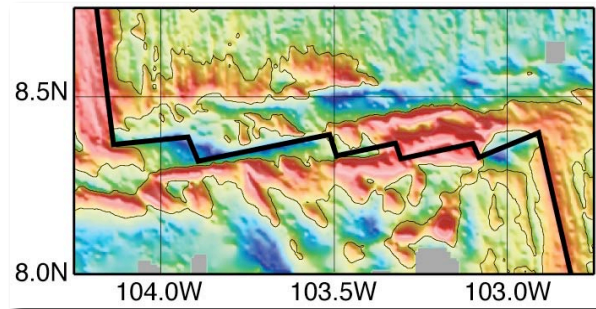
# Conclusions

**Segmentation of oceanic transform faults is VERY important.**

- Earthquake processes
- Fault structure
- Mantle flow and melt extraction

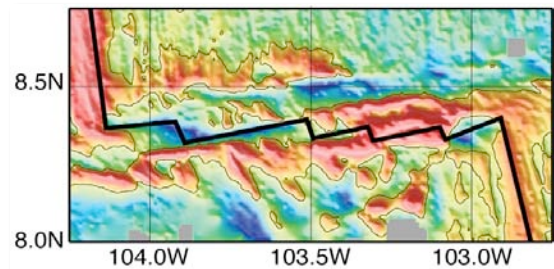


Textbook transform fault:  
Single fault strand!



Natural transform fault:  
Segmented!

# Conclusions



**Segmentation of oceanic transform faults is VERY important.**

1. There is a spreading rate dependence in the gravity anomalies from oceanic transform fault that suggests crustal thickening at several intermediate and fast-slipping transform faults.
2. To explain gravity derived crustal thickness and geochemical variations within Siqueiros transform fault, melt must be pooled from a wide pooling area.